Seed coat formation in Arabidopsis requires a concerted action of JUMONJI histone H3K27me3 demethylases and Brassinosteroid signaling

Rishabh Pankaj[1], Rita B. Lima[1], Guan-Yu Luo[1], Sinah Ehlert[1,2], Pascal Finger[1,2], Hikaru Sato[3] and Duarte D. Figueiredo[1]

[1]Max Planck Institute of Molecular Plant Physiology, Potsdam Science Park, Am Mühlenberg 1, 14476 Potsdam, Germany

[2]Institute of Biochemistry and Biology, University of Potsdam, Karl-Liebknecht-Str. 24-25, 14476 Potsdam, Germany

[3]Department of Integrated Biosciences, The University of Tokyo, Kashiwa, Japan

Abstract

Seed development in flowering plants starts with a double fertilization event where two paternal gametes, the sperm cells, fertilize their maternal counterparts, egg cell and central cell. This leads to the formation of the embryo and the endosperm. These fertilization products are enveloped by the maternally-derived seed coat, the development of which is inhibited prior to fertilization by epigenetic regulator Polycomb Repressive Complex 2 (PRC2). This complex deposits the repressive histone mark H3K27me3, whose removal is necessary for seed coat formation. However, H3K27me3 marks are stable and PRC2 removal does not explain how seed coat genes become activated after fertilization. Here, we show that JUMONJI-type (JMJ) histone demethylases are expressed in the seed coats of *Arabidopsis thaliana* (Arabidopsis) and are necessary for its formation. We further propose that JMJ activity is coupled to Brassinosteroid (BR) function, as BR effectors have been shown to physically recruit JMJ proteins to target loci. Consistent with this hypothesis, we show that loss of BR function leads to seed coat defects, which can be rescued by depletion of H3K27me3. Finally, we reveal an additional pathway through which BRs directly regulate seed coat development, independently of H3K27me3 deposition. This discovery highlights the diverse functions of BRs in coordinating seed development, beyond their known roles in plant growth and development.

Introduction

Changes in chromatin structure via epigenetic modifications, including DNA methylation and histone marks, modulate gene expression and thus shape plant and animal development. Plants have extensive systems in place to control the deposition and removal of these epigenetic marks on their chromatin (Hemenway and Gehring, 2023). Among such marks, H3K27me3 is a critical histone modification that induces gene repression and chromatin compaction (Mozgova et al., 2015). This mark is deposited by Polycomb Group proteins (PcG), which form multimeric complexes known as POLYCOMB REPRESSIVE COMPLEXES (PRC). This includes complexes of the PRC1 and PRC2 types, the latter being responsible for H3K27me3 deposition. In the model system *Arabidopsis thaliana* (Arabidopsis), there are three PRC2 complexes, each with its unique collection of components and roles in plant growth: EMBRYONIC FLOWER (EMF), VERNALIZATION (VRN), and FERTILIZATION-INDEPENDENT SEED (FIS). The EMF- and VRN-PRC2s are specific to the sporophytic generation, while FIS-PRC2 is specific to the gametophyte and to one of its products, the endosperm (Mozgova et al., 2015).

The developing seed of an angiosperm contains three genetically distinct structures: embryo, endosperm, and seed coat. While the formation of the first two is directly linked to the fertilization of the egg cell and of the central cell, the seed coat, which derives from the ovule integuments, is not a direct product of fertilization. This has two implications: 1) seed coat development is blocked prior to fertilization, and 2) the ovule integuments require a signal coming from the fertilization products, to drive seed coat formation. Indeed, the development of the seed coat is actively blocked prior to fertilization by the sporophytic PRC2s, EMF and VRN (Roszak and Köhler, 2011). Moreover, the hormone auxin is the signal coupling fertilization to seed coat development (Figueiredo et al., 2016). Following fertilization, the endosperm produces auxin (Figueiredo et al., 2015), which is then transported to the integuments, where it removes the PRC2s, allowing for seed coat development (Figueiredo et al., 2016). In summary, sporophytic PRC2s are responsible for restricting seed coat formation before fertilization and this block is lifted by auxin. This is supported by the observation that mutants lacking sporophytic PRC2 activity, and thus have reduced levels of H3K27me3, produce fertilization-independent (or autonomous) seed coats (Figueiredo et al., 2016; Roszak and Köhler, 2011). This is the case for mutants lacking the PRC2 components SWINGER (SWN), CURLY LEAF (CLF), VERNALIZATION 2 (VRN2) and EMBRYONIC FLOWER 2 (EMF2). Genes encoding these PRC2 subunits are downregulated upon fertilization or upon exogenous application of auxin (Figueiredo et al., 2016). Concurrently, treating ovules with exogenous auxin leads to autonomous seed coat formation, as auxin removes

PRC2 function (Figueiredo et al., 2016). However, the auxin-derived removal of PRC2 does not explain how seed coat genes become active, given that the H3K27me3 marks should be stable. Importantly, seed coat growth is not driven by cell division but by cell elongation (Figueiredo et al., 2016), meaning that dilution of the marks is unlikely. Therefore, the H3K27me3 marks must likely be actively removed following fertilization, but the enzymes responsible for this process are still unknown.

Histone demethylases, such as those containing JumonjiC domains (JmjC), can remove histone marks such as H3K27me3. Arabidopsis has 21 predicted JmjC proteins that can be categorized into five classes based on the architecture of their protein domains (Crevillén, 2020). While not all members have been fully studied, they include potential H3K9me3, H3K36me3, H3K4me3, and H3K27me3 demethylases. In Arabidopsis, five H3K27me3 demethylases have been identified so far, including two JmjC domain-only proteins, JUMONJI 30 (JMJ30/AtJMJD5) and JUMONJI 32 (JMJ32), as well as three C2H2-type zinc-finger (ZnFn)-containing JmjC proteins, EARLY FLOWERING 6 (ELF6/JMJ11), RELATIVE OF ELF6 (REF6/JMJ12), and JUMONJI 13 (JMJ13) (Crevillén et al., 2014; Cui et al., 2016; Gan et al., 2014; F. Lu et al., 2011; S. X. Lu et al., 2011; Yan et al., 2018). However, it is possible that additional H3K27me3 demethylases are yet to be discovered. The three major H3K27me3 demethylases REF6, ELF6 and JMJ13 have been shown to be important for reproductive processes. REF6 was shown to be necessary for suppression of the seed dormancy (Chen et al., 2020), as well as for seed germination (Pan et al., 2023; Sato et al., 2021; Yahan Wang et al., 2023). ELF6 and JMJ13, on the other hand, have been shown to control carpel growth in an antagonistic matter (Keyzor et al., 2021). ELF6 was also shown to be expressed in the mature ovules and in the embryo (Crevillén et al., 2014; Yang et al., 2016). Finally, JMJ13 has been shown to be necessary for genome-wide H3K27me3 demethylation in the pollen (Borg et al., 2020).

Although JMJs play key roles in epigenetic reprogramming, these proteins often must be recruited to their target loci by transcription factors (TF). This includes TFs involved in brassinosteroid (BR) signaling, like BRASSINAZOLE-RESISTANT 1 (BZR1) and BRI1-EMS-SUPPRESSOR 1 (BES1) (Li et al., 2018; Yu et al., 2008). As hormones of steroid nature, BRs serve a variety of roles in plant development (Manghwar et al., 2022). They control cell division, stem cell maintenance, vascular development, cell elongation, root growth and floral transition, among other processes (Fàbregas and Caño-Delgado, 2014; Lv et al., 2018; Singh and Savaldi-Goldstein, 2015; Vukašinović et al., n.d.; Wang et al., 2020). Moreover, several studies have demonstrated the importance of BRs in seed development. For example, the rice BR biosynthesis mutants *brd2* and

dwf11 produce smaller seeds (Hong et al., 2005; Tanabe et al., 2005). Furthermore, the rice dwarf mutant *d61* also produces small seeds, which is due to the loss of function of a rice BR receptor, encoded by *OsBRI1* (BRASSINOSTEROID INSENSITIVE 1) (Morinaka et al., 2006). BR deficient *Vicia faba* mutants also make smaller seeds (Fukuta et al., 2006), as does the dwarf pea mutant *lk*, a severe BR deficient mutant (Nomura et al., 2007). Overexpression of a BR-biosynthetic gene, on the other hand, has been demonstrated to boost rice seed filling and yield (Wu et al., 2008). In Arabidopsis, the BR-deficient mutant *dwf5* produces small seeds (Choe et al., 2000), whereas overexpression of the P450 monooxygenase family gene *CYP72C1* in the dwarf mutant background *shk1-D* reduces endogenous BR levels, resulting in general short organs and small seeds (Takahashi et al., 2005). The mature dry seeds of the BR-deficient mutant *deetiolated 2* (*det2*) and the BR-insensitive mutant *bri1-5* (a weak allele of BRI1) were discovered to be smaller than the respective wild-type (WT) seeds (Jiang et al., 2013). Furthermore, exogenous BR was shown to partially rescue *det2* seed size and weight, indicating positive regulatory role for BRs in seed growth (Jiang et al., 2013). The effect of BRs on seed growth was proposed to be determined by the direct regulation of BZR1 of genes involved in endosperm proliferation, such as *SHB1*, *IKU1*, *MINI3*, and *IKU2*, all of which work in the same pathway (Garcia et al., 2003; Luo et al., 2005; Wang et al., 2010; Zhou et al., 2009). Finally, BRs have been proposed to regulate seed number (Jiang and Lin, 2013).

Although BRs have been implicated in regulating seed growth, the underlying molecular mechanisms are still poorly understood. Importantly, as alluded to above, the BR effector BES1 was shown to regulate the expression of target genes by recruiting the JMJ histone demethylases ELF6 and REF6 (Yu et al., 2008). Interestingly, BES1 interacts physically with both ELF6 and REF6 (Yu et al., 2008), while BZR1 interacts with ELF6 but not REF6 (Li et al., 2018). We thus hypothesized that JMJ and BR function could be necessary to remove H3K27me3 marks from the integuments, allowing the seed coat to develop after fertilization. Indeed, here we show that BR and JMJ mutants show seed coat defects. Consistent with our hypothesis that BRs are necessary for H3K27me3 removal, we show that BR mutant phenotypes are rescued by loss of PRC2 function in the integuments. Moreover, we uncover a dual role for BR regulation of seed coat growth, mediated by the main BR receptor BRI1 and by one of its close homologues BRI-LIKE 3 (BRL3).

Results

REF6 and ELF6 H3K27me3 demethylases are expressed in the seed coat

Previous research indicates that seed coat development is blocked by H3K27me3 marks, which are deposited by sporophytic PRC2s. Auxin-mediated removal of the PRC2s is therefore necessary for seed coat formation following fertilization. However, PRC2 removal alone should not be sufficient, because the H3K27me3 marks should be stable in the non-dividing seed coat cells. If this is true, then ovules of mutants partly lacking PRC2 function, and therefore depleted in H3K27me3, should be more responsive to exogenous auxin, and should develop larger autonomous seed coats, when compared to the WT. Indeed, we observed that the sporophytic PRC2 mutant *swn clf/+* produces larger autonomous seeds than Col-0 after treatments with 100 µM of the synthetic auxin 2,4-Dichlorophenoxyacetic acid (2,4-D; **Fig. S1**). This observation supports the hypothesis that removal of H3K27me3 marks in the seed coat after fertilization is an essential step for seed coat growth. We then hypothesized that H3K27me3 marks should be enzymatically removed from the integument cells following fertilization. This process can be carried out by JMJ-type histone demethylases. Therefore, we analyzed previously published seed-specific transcriptomic datasets to test if JMJ encoding genes are expressed in the seed coat (**Fig. S1**). Indeed, several genes encoding H3K27me3 demethylases are predicted to be expressed during seed coat development, including *ELF6*, *JMJ13* and *JMJ30*. Unfortunately, the microarray dataset that we used did not contain a probe for *REF6* (Belmonte et al., 2013).

Because in Arabidopsis the removal of H3K27me3 marks is carried out by three main H3K27me3 demethylases: REF6, ELF6 and JMJ13, we decided to focus our analyses on these members of the JMJ family. Through analysis of a *REF6::REF6:GFP* reporter in a *ref6c* mutant background (Yan et al., 2018), we found that REF6 is expressed in the integuments of unfertilized ovules, as well as in seed coats of 1 DAP seeds (**Fig. 1A**). At these stages of development, no REF6 expression was seen in the gametophyte or in the early endosperm or embryo. We confirmed these observations using a line expressing *REF6::GUS*, and consistently observed GUS activity in sporophytic and zygotic tissues of developing seeds as well as a strong expression in anthers (**Fig. S2**). Regarding ELF6, it was previously found to be expressed in mature ovules as well as in developing embryos (Crevillén et al., 2014). We analyzed a reporter line expressing *ELF6::GUS* and indeed observed GUS activity in the sporophytic tissues of developing seeds (**Fig. 1B**). Finally, we analyzed JMJ13 transcriptional (*JMJ13:GFP*) and translational (*JMJ13:JMJ13-GFP*) reporters and did not observe any *JMJ13* expression in ovules or seeds. To test if these reporters were functional, we checked their expression in developing anthers, as JMJ13 has been shown

164 to be expressed in pollen (Borg et al., 2020). Indeed, fluorescence was observed in mature pollen
165 grains (**Fig. S2**), confirming that the reporters are functional and that JMJ13 is likely not expressed
166 in seeds. These expression results indicate that among the three main H3K27me3 demethylases,
167 REF6 and ELF6 are the ones with the strongest expression in seeds, whereas together with
168 REF6, JMJ13 is mostly expressed in pollen.

Fig 1

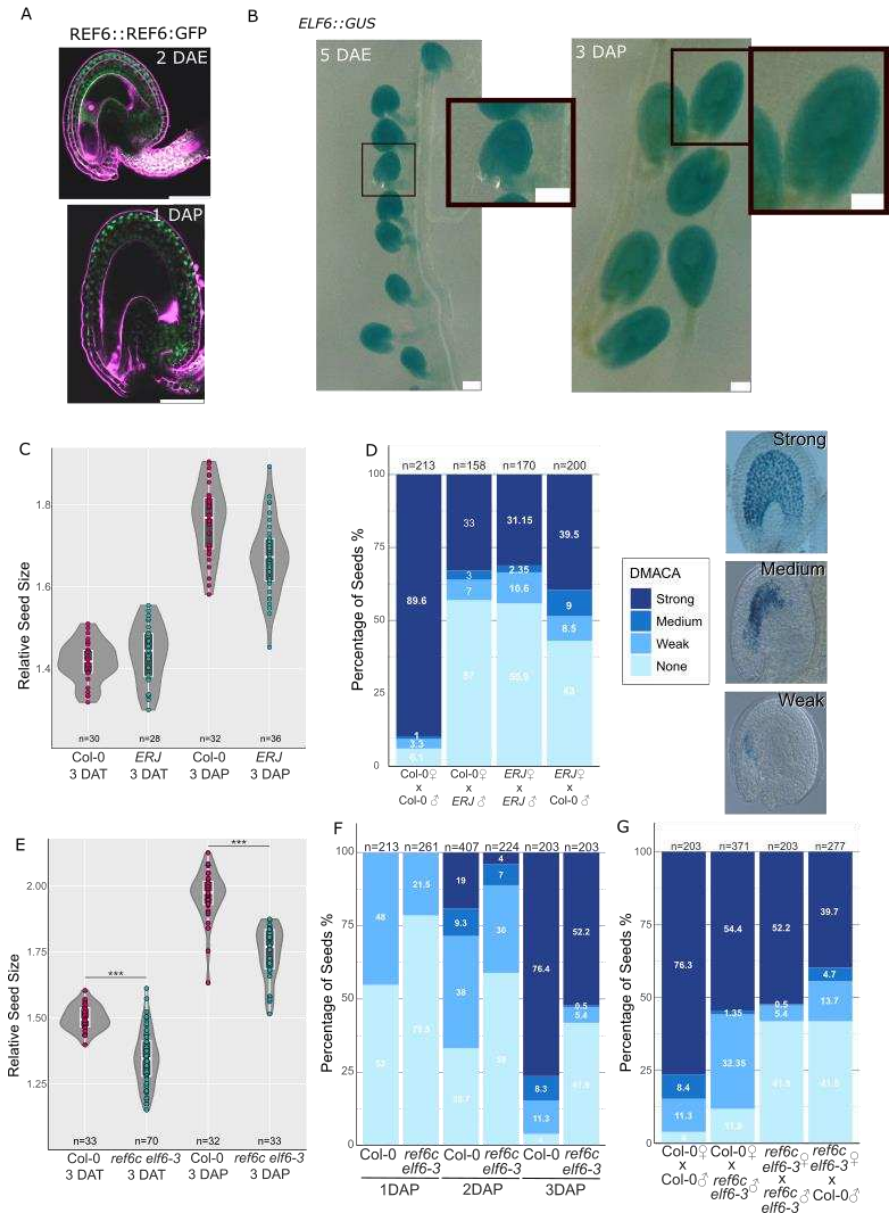

169

170 **Fig. 1. JMJ activity is necessary for seed coat formation.** (**A**) Expression of *REF6::REF6-GFP* in *ref6c*
171 in an unfertilized ovule at 2 days after emasculation (DAE; top) and 1 day after pollination (DAP; bottom).
172 Scale bars indicate 50 µm. Magenta is propidium iodide. (**B**) Expression of *ELF6:GUS* in unfertilized ovules
173 and developing seeds. Scale bars indicate 50 µm. (**C**) Autonomous and sexual seed size of *elf6 ref6c jmj13*

(ERJ) and the respective WT. The relative seed size was calculated as a ratio between the perimeter of each seed and the average perimeter of unfertilized ovules of their respective genotype. (**D**) DMACA staining of *ERJ* x Col-0 reciprocal crosses. The staining was classified in four categories: examples shown on the right hand-side for the three stained categories. (**E**) Autonomous and sexual seed size of *ref6c elf6-3* and the respective WT. The relative seed size was calculated as a ratio between the perimeter of each seed and the average perimeter of unfertilized ovules of their respective genotype. *** Differences are significant for 0.001>p (ANOVA). (**F-G**) DMACA staining of *ref6c elf6-3* at 1, 2 and 3 DAP (**E**), and of *ref6c elf6-3* x Col-0 reciprocal crosses (**F**).

Mutants for JMJ type H3K27me3 demethylases have seed coat development defects

In order to test whether JMJ histone demethylases are responsible for H3K27me3 demethylation in the seed coat, we assessed seed coat formation in *ref6-1, elf6-3* and *jmj13* single mutants. We did this both using sexual and asexual (or autonomous) seeds, using seed size as a proxy for seed coat expansion. Shortly, we compared the size of sexual seeds 3 days after pollination (referred to as 3 DAP) and/or of autonomous seeds 3 days after 100 µM auxin (2,4-D) treatment (referred to as 3 DAT). We selected this time point, because in these early stages of seed development the expansion of the seed is purely driven by seed coat growth and its interactions with the endosperm. For instance, the size of a mature Arabidopsis seed is also determined by the embryo, and therefore we used a timepoint in which the embryo size did not impact on our measurements. The reasoning for analyzing autonomous seeds, as produced via exogenous auxin applications, in addition to sexual seeds, was to test if auxin-induced seed coat formation is specifically impaired in *jmj* mutants.

At 3 DAP we observed that seeds of the single *ef6c, elf6* and *jmj13* mutants were approximately the same size of the corresponding WT (**Fig. S3**). We also did not find consistent differences in the size of autonomous seeds at 3 DAT (**Fig. S3**). This indicates that the *jmj* single mutants do not show any major seed coat initiation defects. Since ELF6, REF6 and JMJ13 share significant homology, it is possible that they redundantly control seed coat formation. Consequently, we analyzed higher order mutants for these genes. We obtained and analyzed a published *elf6 ref6c jmj13 (ERJ)* triple mutant (Yan et al., 2018). Plants carrying these three mutant alleles are dwarf, exhibit delayed flowering time relative to the WT, and show bent siliques, as previously described (**Fig. S4**) (Yan et al., 2018). This was not observed in the single mutants, indeed supporting the idea of functional redundancy between these JMJs. We then conducted a similar comparative analysis of the sizes of sexual and autonomous seeds. Surprisingly, and contrary to our expectations, we found that both sexual and autonomous seeds of the triple mutant were slightly

but significantly larger than those of the wild type (**Fig. S3**). However, we noted that the unfertilized/mock ovules of the triple mutant were also significantly larger than those of the wild type (see mock-treated samples in **Fig. S3**). And thus, when normalizing for the size of unfertilized ovules, we detected a slight, but not statistically significant, reduction in relative seed coat growth in the *ERJ* mutant compared to the WT (**Fig. 1C**). Therefore, we used an alternative approach to assess seed coat formation: we performed DMACA (p-dimethylaminocinnamaldehyde) staining of seeds at 1, 2 and 3 DAP. This dye stains the proanthocyanidins (PAs) produced in the endothelium of the seed coat, and can therefore be used as a visual marker for seed coat development (Debeaujon et al., 2003). Supporting our hypothesis, we observed that seeds of the *ERJ* triple mutant showed a striking delay in the accumulation of proanthocyanidins, when compared to the WT (**Fig. 1D**). This was obvious in all three time points assessed, and fits with our expectation that JMJ function is necessary for seed coat development.

Our analyses also revealed that the siliques of *ERJ* contained many immature ovules or aborted seeds (**Fig. S3 and S4**). There could be several reasons for this: 1) a post-fertilization effect on seed viability; 2) compromised pollen function; or 3) compromised ovule viability. To test if any of these was true, we did DMACA staining of 3 DAP seeds of reciprocal crosses of *ERJ* × Col-0 (**Fig. S3**). This analysis revealed several reproductive defects in the *ERJ* mutant, which results in a reduced number of fertilized seeds. Specifically, we observed that in *ERJ* × Col-0 (by convention the maternal parent is indicated first)**,** 43% of the total seeds in the siliques did not stain with DMACA, even after 3 days. Upon closer inspection we observed that many of these ovules were not fully mature (**Fig. S3**), which led to a lower number of fertilized seeds. Additionally, in Col-0 × *ERJ* crosses we again observed that many seeds did not stain with DMACA, and approximately 57% of ovules were in fact unfertilized. This is likely due to defects in pollen viability. Nevertheless, in *ERJ* × Col-0 crosses, where the seed coat is derived from the triple mutant, a significant proportion of viable seeds (~17.5%) were delayed in seed coat development, as indicated by less DMACA staining compared to their wild-type counterparts (WT; categories “Medium” and “Weak” in **Fig. 1D and S3**). This fits our hypothesis that these JMJs are necessary for seed coat development.

However, despite these findings, the pleiotropic defects of the triple mutant complicated its analysis. To counter this, we analyzed less strong double mutants, and phenotyped seeds of *ref6-1 elf6-3*, *elf6-3 jmj13* and *jmj13 ref6-1*. None of the three double mutants showed any visible vegetative growth phenotypes. Although, when comparing the 3 DAT autonomous seed size phenotype of all three double mutants, we observed that all three mutants produced seeds that

were slightly smaller than the WT ones (**Fig. S3**). Because JMJ13 does not seem to be expressed in seeds, as we describe above, we further focused on ELF6 and REF6 as potential regulators of seed coat development. In the double mutant analysis of **Fig. S3** we used *ref6-1*, which is a knock-down of REF6. Therefore, we obtained and analyzed the stronger *ref6c elf6* mutant, where *ref6c* is a CRISPR-knock-out allele of *REF6* (Yan et al., 2018). Unlike *ref6-1 elf6-3*, the stronger *ref6c elf6* mutant had visible vegetative growth defects: the plants displayed dwarfed growth patterns, similar to those seen in the *elf6 ref6c jmj13* mutants, but did not exhibit their characteristic bent silique phenotype (**Fig. S3 and S4**). Importantly, the *ref6c elf6* double mutant produced young seeds that were smaller than the WT ones, as is expected for mutants with seed coat initiation defects (**Fig. 1E**). This was true both for sexual seeds and for those obtained via exogenous auxin applications. Moreover, the *ref6c elf6* double mutant seeds showed seed coat defects when stained with DMACA (**Fig 1F-G**): *ref6c elf6* produced a significant number of seeds that did not stain with DMACA and, unlike in the WT, the staining did not increase as much in the mutant seeds as they developed (**Fig. 1F**). In fact, around 42% of the *ref6c elf6* seeds did not stain with DMACA even after 3 DAP. To further confirm the origin and nature of the defect, we performed reciprocal crosses of *ref6c elf6* with the WT (**Fig. 1G**). Interestingly, in the case of Col-0 X *ref6c elf6,* the pollen defects seem to be reduced when compared to the *ERJ* triple mutant (**Fig. S3**). This is in line with JMJ13 being specifically expressed in pollen (**Fig. S2**). On the other hand, in the case of *ref6c elf6* × Col-0, the number of immature/aborted ovules persisted (**Fig. 1G**), similar to *ERJ* (**Fig. S3**), suggesting that ovule abortion and seed coat defects are of maternal sporophytic origin. In addition to these findings, it is important to note that *ref6c elf6* mutants still exhibited a decrease in the overall seed set, with only around 30 viable seeds per silique, when compared to around 50 seeds produced by the WT (**Fig. S3**). A reduced seed set normally correlates with larger individual seed size. Therefore, although we observed seed coat development defects in *jmj* mutants, it is possible that the full extent of these defects is partially masked by the low seed set of these lines.

In conclusion, JMJ function is required for seed coat formation. The JMJ H3K27me3 demethylases ELF6 and REF6 are expressed in the seed coat, and mutations in the respective genes lead to delayed seed coat growth and in accumulation of PAs. Additionally, loss of JMJ function also compromises ovule and pollen development, leading to reduced seed sets.

JMJ function represses seed growth at later stages of development in a zygotic manner

Although our data supports a role for H3K27me3 demethylases in promoting seed coat initiation, we were surprised to observe that the *jmj* mutant seeds were actually larger at maturity compared to the respective WT. We tested this in several mutant alleles of *ref6* and *elf6*, as well as for the higher order mutants *elf6-3 ref6c* and *ERJ* (**Fig. 2A and Fig. S4**). Although in the case of the higher order mutants this increase in individual seed size could be due to the reduced seed set, as mentioned above, *ref6* single mutants also produced larger seeds at maturity (**Fig. 2A-B and S4**), although their seed set was comparable to that of the WT (**Fig. S3**). This suggests that JMJ function promotes early seed growth, but represses it at later stages of development. Because REF6 has been shown to have functions in endosperm development (Sato et al., 2021), we hypothesized that the increased size of *ref6* mature seeds could be due to a zygotic effect. To test this, we complemented the *ref6* mutant with constructs driving *REF6* expression under 1) its native promoter, 2) an embryo-specific promoter (*TPS1*) and 3) an endosperm-specific promoter (*EPR1*), as previously described (Sato et al., 2021). As expected, the mature seed size was restored to WT levels when *ref6* was complemented with *REF6::REF6:GFP* (**Fig. 2C**). Importantly, we also observed a partial but significant rescue of the *ref6* mature seed size phenotype in lines expressing *TPS1::REF6* and *EPR1::REF6* (**Fig. 2D**). This suggests that the increased size of *jmj* mutant seeds is, at least in part, due to zygotic effects of the embryo and the endosperm. If this is true, then REF6 should target genes that are specifically expressed in all three seed tissues. We thus searched for REF6 binding sites in embryo-, endosperm- and seed coat-specific genes, based on published datasets (Belmonte et al., 2013; Cui et al., 2016). Indeed, 326 genes bearing at least four REF6 binding motifs CTCTGYTY in their vicinity are specifically expressed in the three seed tissues (**Fig. 2E** and **S5**). Interestingly, there is little overlap between REF6 targets in those tissues, suggesting that REF6 controls different biological processes in the different tissues, and at different developmental timepoints. Thus, our data points to a sporophytic function of JMJs at early stages of seed development, promoting seed coat formation, and to a zygotic function at later stages of seed development, restricting embryo and endosperm growth. Consistent with this, *REF6* is strongly expressed in the seed coat in the first days of seed development, but its expression decreases in this tissue as the seeds develop (**Fig. S2**). By day 6 after pollination (6 DAP in **Fig. S2**) *REF6:GUS* expression is mostly absent from the seed coat and mostly detectable in the zygotic products.

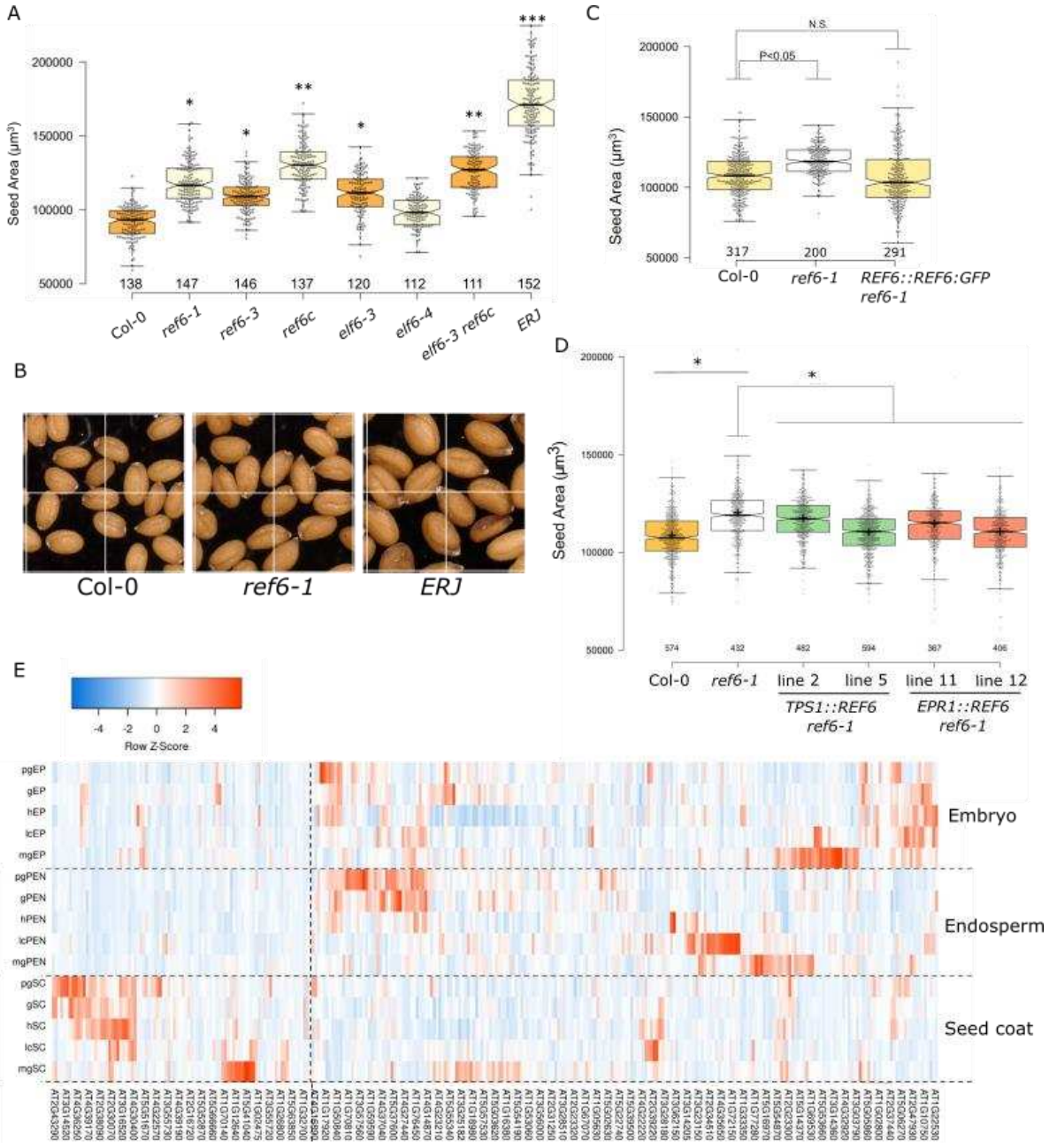

Fig. 2. Zygotic effect of JMJs in mature seed growth. (**A**) Seed area of mature seeds of WT, *ref6* and *elf6* single mutants, and higher order JMJ mutants. Examples of seeds can be seen in (**B**) and in **Fig. S4**. (**C-D**) Mature seed area of WT, *ref6-1* and *ref6-1* complemented with the endogenous *REF6::REF6:GFP* (**C**), or with embryo (*TPS1*) or endosperm (*EPR1*) specific promoters (**D**). Two independent transgenic lines are shown. * indicates statistical significance for p<0.01 (Tukey multiple comparison) (**E**) Relative expression of genes carrying predicted REF6 binding sites, specifically expressed in the embryo proper (upper panel), peripheral endosperm (middle panel) and seed coat (lower panel). Extended dataset can be found in **Fig. S5**. The seed stages indicated are: pg, pre-globular; g, globular; h, heart; lc, linear cotyledon; and mg, mature green.

BR mutants are defective in seed coat development

Given our observation that ELF6 and REF6 are redundantly required for seed coat formation, and given that both H3K27me3 demethylases have been shown to interact with the BR effectors BES1 and BZR1, we hypothesized that BR function could be required in the seed coat for H3K27me3 removal. We checked previously published datasets (Belmonte et al., 2013), and indeed genes involved in BR biosynthesis and signaling are strongly expressed in the seed coat (**Fig. 3A**). We recently confirmed that this is the case and all known enzymes involved in BR biosynthesis, as well as the BR receptor BRI1, co-receptor BAK1 and effectors BZR1 and BES1 are all specifically expressed in the early seed coat (Lima et al., 2023).

If our hypothesis is true, that BR signaling is required for H3K27me3 removal via JMJ function during seed coat formation, then BR-related mutants should show defects in seed coat development. Thus, we examined previously published BR mutants for seed defects. We tested loss-of-function mutants for components of BR signaling and biosynthesis. Indeed, we observed that mutants lacking the main BR receptor BRI1 form seeds that are significantly smaller than those of WT at 3 DAP (**Fig. 3B-D**). The same is true for mutants impaired in BR biosynthesis like *br6ox1 br6ox2* and *det2-1* (**Fig. 3D,E**). Similar to what we did for the JMJ mutants, we also analyzed the size of auxin-induced autonomous seeds. Again, we observed that all tested BR mutants initiate smaller autonomous seed coats, when compared to the WT (**Fig. S6**). For further experiments we selected one BR biosynthetic mutant, *det2-1*, and one signaling mutant, *bri1-6*. Importantly, the size of unfertilized ovules of *det2* and *bri1* plants was not significantly different from that of the wild type (**Fig. S6**), which signifies that the delay in seed growth is due to pathways that are activated after fertilization and not to initial ovule size. Overall, since the expression of BR genes is restricted to the seed coat, the smaller seed size in these mutants is likely a result of defects in seed coat development and not from a non-cell autonomous effect of the endosperm or embryo. Further evidence of this was obtained by expressing PHYB ACTIVATION TAGGED SUPPRESSOR 1 (BAS1), a protein responsible for degrading bioactive BRs (Turk et al., 2005), specifically in the seed coat. We observed that 4 out of 9 independent transgenic lines expressing the construct *KLUH:BAS1* produced seeds smaller than the WT control (**Fig. S6**). The promoter of *KLUH* is specific to the sporophytic tissues of the seed (Adamski et al., 2009). The effect was not as strong as what we observed for BR mutants, which is likely the result of the *KLUH* promoter not being expressed in all integument layers.

To further validate these results, we treated WT seeds with propiconazole, a known BR biosynthesis inhibitor (Hartwig et al., 2012). We applied 200 µM of propiconazole 6 h after

pollination, to allow fertilization to take place. We observed that 3 DAP seeds treated with propiconazole were smaller than mock treated seeds (**Fig. S6**). This further confirms that BR function is necessary for seed coat growth.

Fig 3

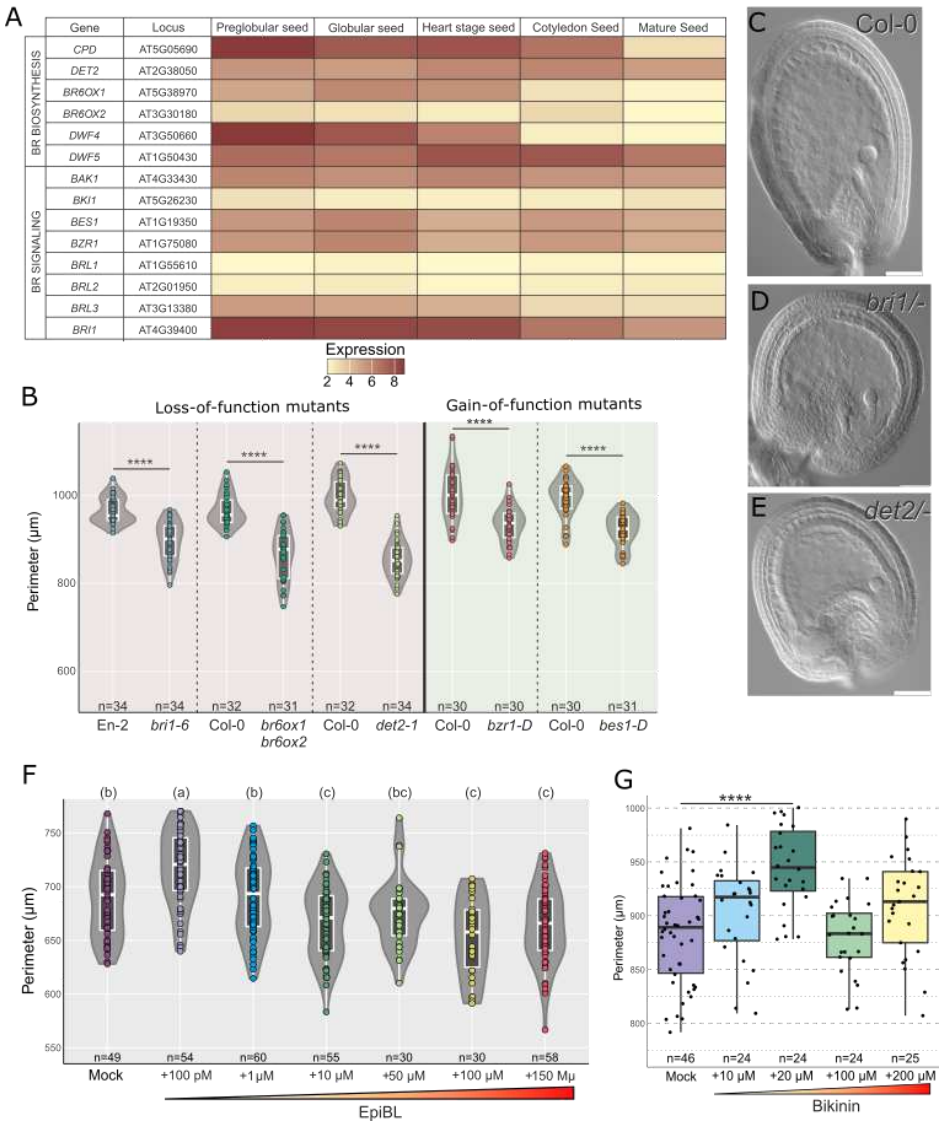

Fig. 3. BR levels impact on seed coat development. (**A**) Relative expression of genes involved in BR biosynthesis and signaling in the seed coat, at different stages of seed development (indicated above), as determined in (Belmonte et al., 2013). (**B**) Perimeter of seeds at three DAP for loss- and gain-of-function BR mutants. The morphology of the seeds can be seen in **C-E**, for WT, *bri1* and *det2*. Scale bars indicate 50 µM. (**F-G**) Perimeter of 3 DAT autonomous seeds after exogenous application of 100 µM 2,4-D and varying concentrations of epi-brassinolide (EpiBL; **F**) or bikinin (**G**). **** represents p-value <0.0001 (Anova, **B**, **G**). For **F**, the letters on top indicate statistical significance for p-value <0.01 (Anova).

Exogenous BRs show a dose-dependent effect on seed size

We then tested the effects of constitutive BR biosynthesis or signaling in seed coat growth. For this, we analyzed several gain-of-function BR mutants. Our expectation was that those mutants would produce larger seed coats, when compared to the WT. We tested the mutant *dwf4-5D*, in which a T-DNA carrying a *CaMV35S* enhancer is inserted in the promoter of the BR biosynthesis gene *DWARF4* (*DWF4*), resulting in a constitutive production of BRs. Our results showed that the 3 DAP and mature seeds of this mutant were significantly larger than those of the WT, although we did not observe the same trend in auxin-induced autonomous seeds (**Fig. S6**).

We then analyzed *bes1-D* and *bzr1-D* mutants, which are constitutive BR signaling mutants. Both alleles result from a single nucleotide change in the coding region which prevents BES1/BZR1 phosphorylation by BIN2, resulting in constitutive accumulation of these transcription factors in the nucleus (Wang et al., 2002; Yin et al., 2002). Unexpectedly, our results showed that 3 DAP seeds of *bes1-D* and *bzr1-D* mutants were smaller than those of WT (**Fig. 3B**). We also observed similar results for autonomous seeds (**Fig. S6**). These findings suggest that, although BR function is required for seed coat formation, excessive BR signaling has a detrimental effect on development. Thus, BRs seem to affect the seed coat development in a dose development manner.

To further verify this, we performed exogenous treatments of WT ovules with epi-brassinolide (epi-BL), a bioactive BR. We treated the unfertilized ovules in a similar manner as we did for the exogenous auxin treatments. First, to test if BRs induce autonomous seed coat formation, we treated emasculated flowers of Col-0 with different concentrations of epi-BL (100 pm, 1 µM, 10 µM, 100 µM and 150 µM). However, we did not see any significant effect of epi-BL on the treated unfertilized ovules (data not shown). To further investigate whether exogenous BRs would have an effect on seed coat development, we repeated this experiment, but treated the ovules with epi-BL one day after an exogenous application of 100 µM 2,4-D. Our results revealed that different concentrations of epi-BL had varying effects on seed size: the ovules treated with 100 µM 2,4-D plus 100 pM epi-BR were slightly but significantly larger than those treated with auxin alone, while ovules treated with concentrations equal or above 10 µM of epi-BL were smaller in size compared to the auxin control (**Fig. 3F**). These results indicate that BR alone is not sufficient to promote autonomous seed development, unlike auxin, but rather that ovules need to be “primed” first by auxin, and that further development is then under BR control. These results also support the hypothesis that BRs affect seed growth in a dose-dependent manner, where low concentrations of epi-BL have a positive effect on seed coat development, but concentrations above a certain

threshold lead to detrimental effects on seed growth. A similar observation was made when we treated 1 DAP pollinated siliques with Bikinin, a synthetic chemical which activates BR signaling by inhibiting BIN2 (Rybel et al., 2009). We treated the siliques 1 day after pollination with 10 µM, 20 µM, 100 µM and 200 µM of bikinin. The seed size peaked at the 20 µM bikinin treatments, and higher concentrations lead to inhibition of seed coat expansion (**Fig. 3G**). These observations support a dose-dependent effect of BR in seed coat growth, which fits with similar observations made in roots (Vukašinović et al., 2021) and endosperms (Lima et al., 2023).

Seed coat defects in BR mutants are of sporophytic origin

To further verify the origin of the seed coat defects in BR mutants, we compared seed size at 3 DAP in homozygous vs heterozygous mutants. The logic behind this experiment is that if the effect in BR mutants is sporophytic in origin, the heterozygous mutant seeds should behave phenotypically like WT, since the seed coats in heterozygous mutants are diploid and still carry a WT allele. While if the effect in the BR mutant is zygotic, then in a heterozygous condition 25% of seeds will carry mutant embryos and endosperms, and we should see a measurable effect in the phenotype. Along with *bri1* and *det2*, we also used the stronger *dwf4-44* BR biosynthesis mutant for this experiment. The *dwf4-44/-* mutant is extremely dwarf and has severe ovule defects, which prevents its use for reproductive studies in the homozygous state. But *dwf4-44/+* mutants are phenotypically similar to WT, and produce full seed sets. Our results showed that while seeds of the homozygous *bri1* and *det2* mutants are significantly smaller than WT, as we demonstrated above, the seeds of heterozygous *bri1/+*, *det2/+* and *dwf4-44/+* mutants are indistinguishable from WT (**Fig. 4A-D**). Together with the observation that BR genes are specifically expressed in the sporophytic tissue of seeds (Lima et al., 2023), these results indicate that the small size of BR mutant seeds is due to a seed coat defect.

To further confirm this, we generated tissue-specific rescue constructs to complement the BR mutants. Namely, we complemented the *bri1* and *det2* mutants by expressing the respective genes under the following promoters: *DD65*, specific to the central cell and early endosperm (Steffen et al., 2007); *BANYULS* (*BAN*), specific to the endothelium of the inner integument (Debeaujon et al., 2003); and *KLUH*, which is expressed in several integument and seed coat layers (Adamski et al., 2009). Importantly, although *KLUH* is expressed in many vegetative tissues, in seeds it is specific to the seed coat at the stage at which we carried out our experiments. Finally, we used the promoter of *Rps5a* (Maruyama et al., 2013), which is

constitutively expressed. The *BRI1* and *DET2* coding sequences were cloned under the control of all these promoters and were transformed into *bri1* and *det2* mutants, respectively.

We observed that in the case of *bri1*, several complementation lines showed a rescue of the seed coat growth phenotype. Out of four lines each expressing either *BAN::BRI1* or *KLUH::BRI1* in *bri1*, all of them exhibited rescue, i.e., the 3 DAP seed size was restored to WT levels (**Fig. 4F**). This is interesting because *BAN* is only expressed in the innermost layer of the integuments, as compared to *KLU*, which has a broader expression. Native BRI1 is expressed more strongly in the outer integument than in the inner integument (**Fig. S7**) (Lima et al., 2023). This means that restoration of BRI1 expression in one of the integument layers is to some degree sufficient to rescue the *bri1* phenotype. Fitting with the gametophyte-specific expression of *DD65*, two out of three lines expressing *DD65::BRI1* in *bri1* did not show a rescue of the phenotype (**Fig. 4F**). And, although one line expressing *DD65::BRI1* did produce bigger seeds, the difference was not statistically significant compared to *bri1*. Finally, as expected, all lines expressing *Rps5A:BRI1* showed a rescue of seed size of the *bri1* mutant (**Fig. 4F**).

The same tissue-specific complementation approach was carried out for *det2*. Again, we observed a rescue of the *det2* seed growth defects in eight out of nine lines expressing *BAN::DET2* and *KLUH::DET2* (**Fig. 4G**). This indicates that restoring BR biosynthesis in the sporophytic tissues is sufficient to rescue the *det2* seed defects. However, it is interesting to point out a particularity about the rescue of *det2* in *BAN::DET2*-expressing lines: endogenous *DET2* is expressed in the outer integument layers (**Fig. S7**) (Lima et al., 2023), but *BAN::DET2* is only expressed in the innermost layer of the integuments (endothelium). Thus, this rescue implies that BR intermediates, produced in inner integuments, can move to outer integument layers, where enzymes that catalyze the next steps of the pathway are located (Lima et al., 2023). This is unexpected because the inner and outer ovule integuments are not connected symplastically (Stadler et al., 2005) and BRs have been reported to move via plasmodesmata (Wang et al., 2023). Finally, one out of three *DD65::DET2* lines also showed a rescue of the *det2* phenotype (**Fig 4G**). Again, this was surprising given that the *DD65* promoter is specific to the central cell and to the early endosperm, which are symplastically isolated from the seed coat (Stadler et al., 2005). This observation together with the one described above, where the *bri1* phenotype was rescued in one line expressing *DD65:BRI1* might be a sign of non-specific expression of *DD65*. Or alternatively, BR intermediates can cross the endosperm-seed coat barrier and complement the lack of a functional *DET2* in the seed coat of *det2* mutants. In conclusion, our data supports a sporophytic mode of action for seed-produced BRs.

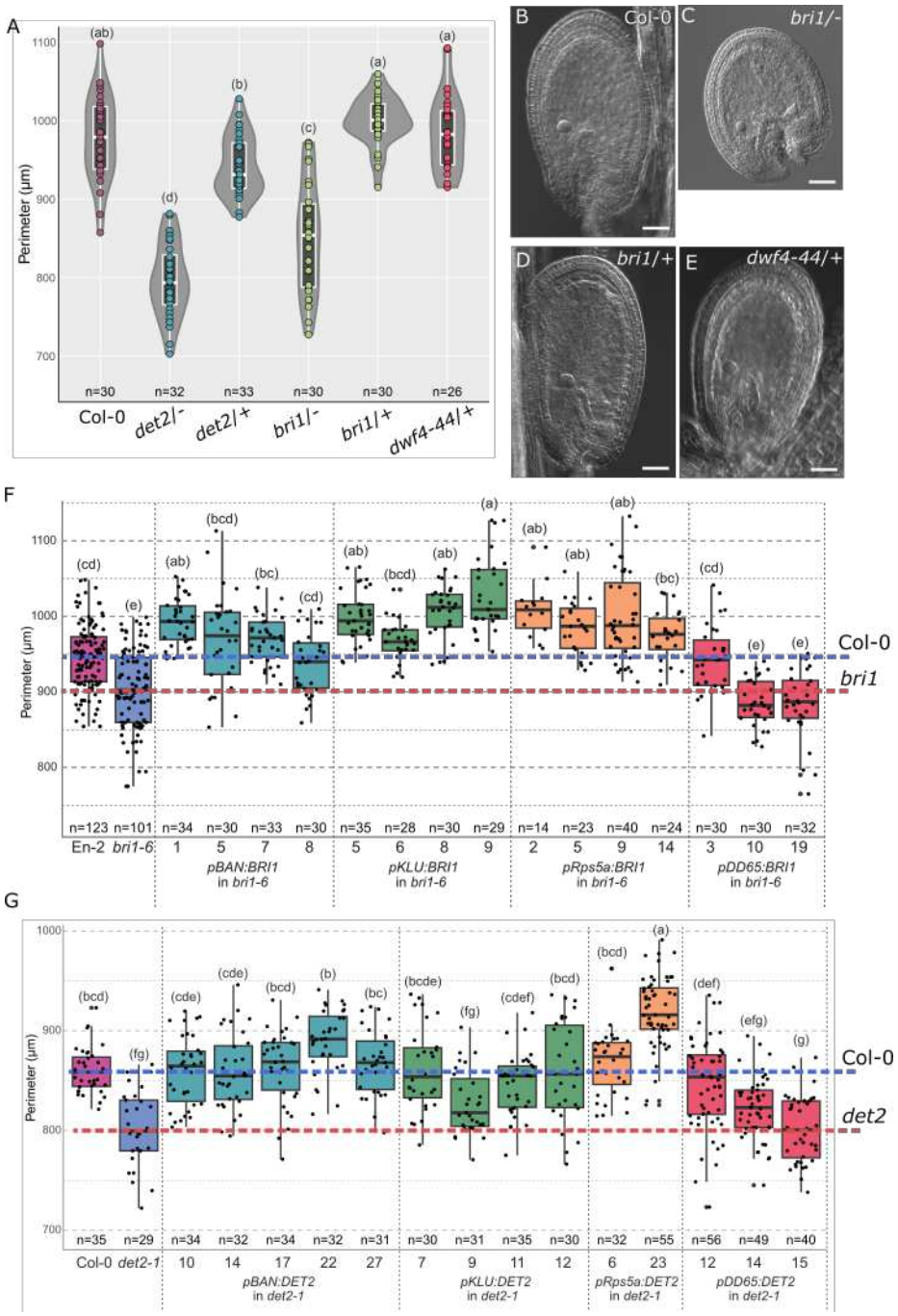

Fig. 4. Sporophytic BRs modulate seed coat growth: (**A**) Seed perimeter of WT, *det2/-, det2/+, bri1/-, bri1/+* and *dwf4-44/+* 3 DAP seeds. Seed morphologies can be seen in **B-E** for WT, *bri1/-*, *bri1*/+ and *dwf4-44*/+, respectively. Scale bars indicate 50 µm. (**F-G**) Perimeter of 3 DAP seeds of *bri1-6* (**F**) and *det2-1* (**G**) and respective complementation lines. All lines are in the *bri1-6* or *det2-1* mutant backgrounds. The phenotypes of the WT and mutants are indicated by the blue and red dashed lines, respectively. The letters indicate statistical significance for p-value <0.05 (Anova).

BR function during seed coat formation is linked to deposition of H3K27me3

Because BR effectors have been shown to recruit ELF6 and REF6 to target loci (Li et al., 2018; Yu et al., 2008), we hypothesized that BR function during seed coat formation could be linked to altered dynamics of H3K27me3. To test if BR effectors and JMJ H3K27me3 are acting in the same pathway during seed formation, we crossed the dominant BR signaling mutant *bzr1-d* to a line ectopically expressing *CaMV35S::ELF6* (Keyzor et al., 2021). However, we observed a high penetrance of aborted and malformed ovules in the double mutant (**Fig. S8**). This was not observed in the single mutants, indicating that indeed BR signaling and H3K27me3 demethylases work in the same pathways during reproductive development. However, this also meant that the double gain-of-function mutants form very few viable seeds and are therefore not useful for functional studies. Thus, as an alternative, we focused on the analysis of sporophytic PRC2 mutants, which lack H3K27me3 marks. Loss of PRC2 function in the ovule integuments, such as in a *swn clf*/+ mutant, leads to autonomous seed coat growth (Figueiredo et al., 2016; Roszak and Köhler, 2011). This is because seed coat development pathways are ectopically activated when H3K27me3 is depleted in the ovule integuments. If we hypothesize that BR function during seed coat development is linked to removal of H3K27me3, then *swn clf*/+ mutants should be insensitive to exogenous applications of epi-BL, as they already lack the repressive epigenetic marks. Indeed, we observed little to no effect of exogenous epi-BL applications on *swn/- clf/+* seed size, unlike what happens in the WT (**Fig. 5A**). These results suggest that due to the lack of H3K27me3 marks in *swn/- clf/+* mutants, seed coat growth genes are expressed independently of fertilization and, therefore, BR levels do not affect seed growth.

Moreover, if our hypothesis is true that BR function in the seed coat is necessary for the efficient removal of H3K27me3 marks by JMJs, then we expect that the seed coat defects of BR mutants are alleviated by loss of PRC2, because those epigenetic marks are not deposited to start with. To further investigate the epigenetic control of seed coat by BRs, we crossed the sporophytic PRC2 mutant *swn/- clf/+* with BR loss-of-function mutants. Interestingly, in the case of *swn/- clf/+ bri1/-* we observed that the triple mutant plants displayed some rescued plant morphologies compared to the *bri1* plants. The triple mutant had larger and more leaves, grew taller (**Fig. 5B**), and flowered later but also for a longer time than *bri1* plants. Importantly, we also observed a similar rescue of the *bri1* growth defects in sexual and autonomous seeds (**Fig. 5C-D and S8**). In fact, seeds of *swn/- clf/+ bri1/-* were of the same size of those of *swn/- clf/+* mutants, resulting in a complete rescue of the growth phenotype and demonstrating that loss of PRC2 is epistatic to the loss of BR signaling via BRI1. Additionally, we observed that the unfertilized ovules of *swn/-*

clf/+ bri1/- were of the same size as those of WT and *bri1/-*, but smaller than those of *swn/- clf/+* (**Fig. S8**). This suggests that lack of BRs to some degree may repress the development of autonomous seed coats in *swn/- clf/+*, potentially because of inefficient removal of residual H3K27me3.

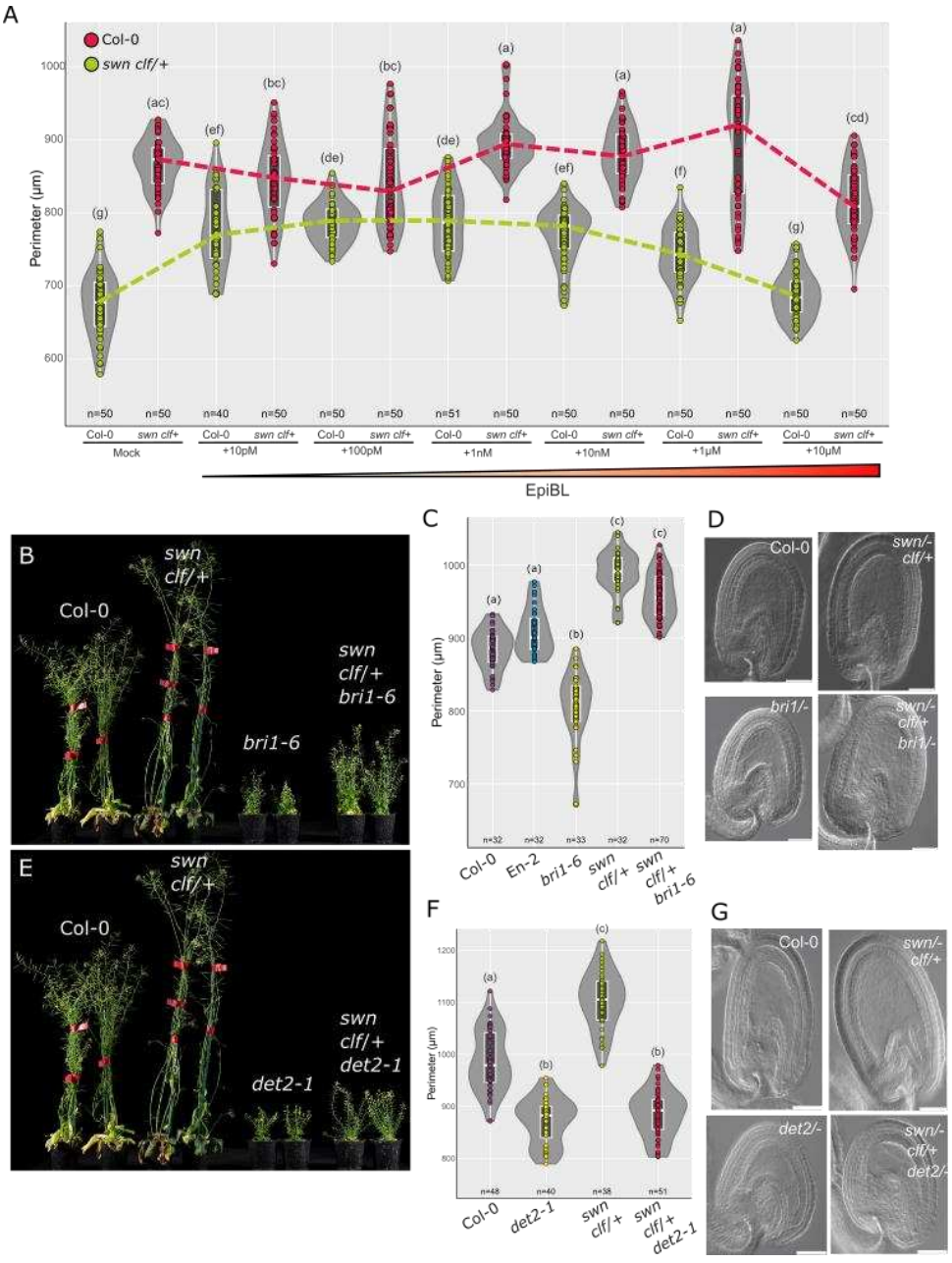

Figure 5. Genetic interactions between PRC2 and BR machinery. (**A**) Seed perimeter of Col-0 (green) and *swn/- clf/+* (red) autonomous seeds at 3 DAT after application of 100 µM 2,4-D and varying concentrations of Epi-BL. (**B**) Vegetative phenotypes of WT, *swn/- clf/+*, *bri1-6* and corresponding triple mutant. (**C**) Seed perimeter at 3 DAP of WT, *swn/- clf/+*, *bri1-6* and corresponding triple mutant. (**D**)

Autonomous seed morphologies of WT, *swn/- clf/+*, *bri1-6* and *swn/- clf/+*, *bri1-6*. Scale bars indicate 50 µm. (**B**) Vegetative phenotypes of WT, *swn/- clf/+*, *det2-1* and corresponding triple mutant. (**C**) Seed perimeter at 3 DAP of WT, *swn/- clf/+*, *det2-1* and corresponding triple mutant. (**D**) Autonomous seed morphologies of WT, *swn/- clf/+*, *bri1-6* and *swn/- clf/+*, *det2-1*. Scale bars indicate 50 µm. The letters in (**A,C,F**) indicate statistical significance for p-value <0.05 (Anova).

Next, we did the same experiment but using the *det2* BR biosynthesis mutant. Surprisingly, the outcome was different from that obtained for *swn/- clf/+ bri1*/-. While we did observe some rescued plant morphologies in *swn/- clf/+ det2/-*, this was not as striking as for *swn/- clf/+ bri1/-* (**Fig. 5B,E**). Moreover, unlike for *bri1*/-, loss of PRC2 function did not rescue the seed growth phenotype of *det2*/-, either in fertilized or auxin-induced autonomous seeds (**Fig. 5F-G and S8**). This suggests that the epigenetic control of seed coat development through BRs might function through multiple pathways, some independent of the main receptor BRI1. To further validate this, we crossed the *swn/- clf/+* mutant to another BR biosynthesis mutant, *dwf4-102/+*. Homozygous mutants for *dwf4-102/-* are severely dwarf and cannot be used for reproductive studies. However, heterozygous *dwf4-102/+* mutants are haplo-insuficient and their 3 DAT seeds are smaller than those of the WT (**Fig. S8**). Importantly, similar to what we observed for *det2*, loss of sporophytic PRC2 did not result in a rescue of the *dwf4-102*/+ phenotype (**Fig. S8**). This indicates that, unlike what happens for BR signaling via BRI1, loss of BR biosynthesis is epistatic to loss of PRC2 and, thus, of H3K27me3.

These observations suggest that loss of BR biosynthesis affects seed coat expansion through pathways both dependent and independent of H3K27me3 removal. One of these pathways could be through BRI1-LIKE receptors (BRLs). There are three BRL receptors in Arabidopsis, of which only two bind bioactive BRs (Caño-Delgado et al., 2004). Based on published gene expression data, only *BRL3* is expressed in the seed coat (**Fig. 6A**). To confirm this, we generated a *BRL3::NLS:tdtomato* reporter line and observed that *BRL3* is strongly expressed in the chalazal seed coat (**Fig. 6B**). Then, to investigate if BR signaling through BRL3 could be involved in seed coat formation, we analyzed 3 DAT and 3 DAP seeds in a *brl3/-* mutant. Indeed, both autonomous and fertilized seeds were significantly smaller in the mutant than in the WT (**Fig. 6C**), despite *brl3/-* mutant plants looking phenotypically similar to WT.

Next, to test if the regulation of seed coat formation by BRL3 is also related to the removal of H3K27me3 marks, we crossed the *swn/+ clf*/- mutant with *brl3* to examine whether the *swn/- clf/+ brl3/-* triple mutants exhibits any rescue in seed size as observed for *swn/- clf/+ bri1/-* (**Fig. 5C**). Surprisingly, we only observed a slight rescue of the *brl3*/- seed phenotype in *swn/- clf/+ brl3/-* for

both sexual and autonomous seeds (**Fig. 6D and S8**). Although the *swn/- clf/+ brl3/-* triple mutant seeds were bigger than those of the *brl3/-* single mutant, they were only as large as WT seeds. And nowhere near those of the *swn/- clf/+* double mutant, which is what we observed in the case of *bri1* (**Fig. 5C**). This observation is interesting because BRI1 and BRL3 are both homologous BR receptors, but they seem to have different functions when it comes to seed coat growth.

We thus propose a model where BR signaling and H3K27me3 removal by JMJ histone demethylases work in a coordinated manner to allow seed coat development. In it, BR signaling through the main receptor BRI1 is necessary for seed coat formation in a manner dependent on H3K27me3 removal, likely through recruitment of ELF6 and REF6 by BR effectors. While signaling through BRL3 is also necessary for seed coat growth, but in a manner independent of H3K27me3 removal (**Fig. 6E**).

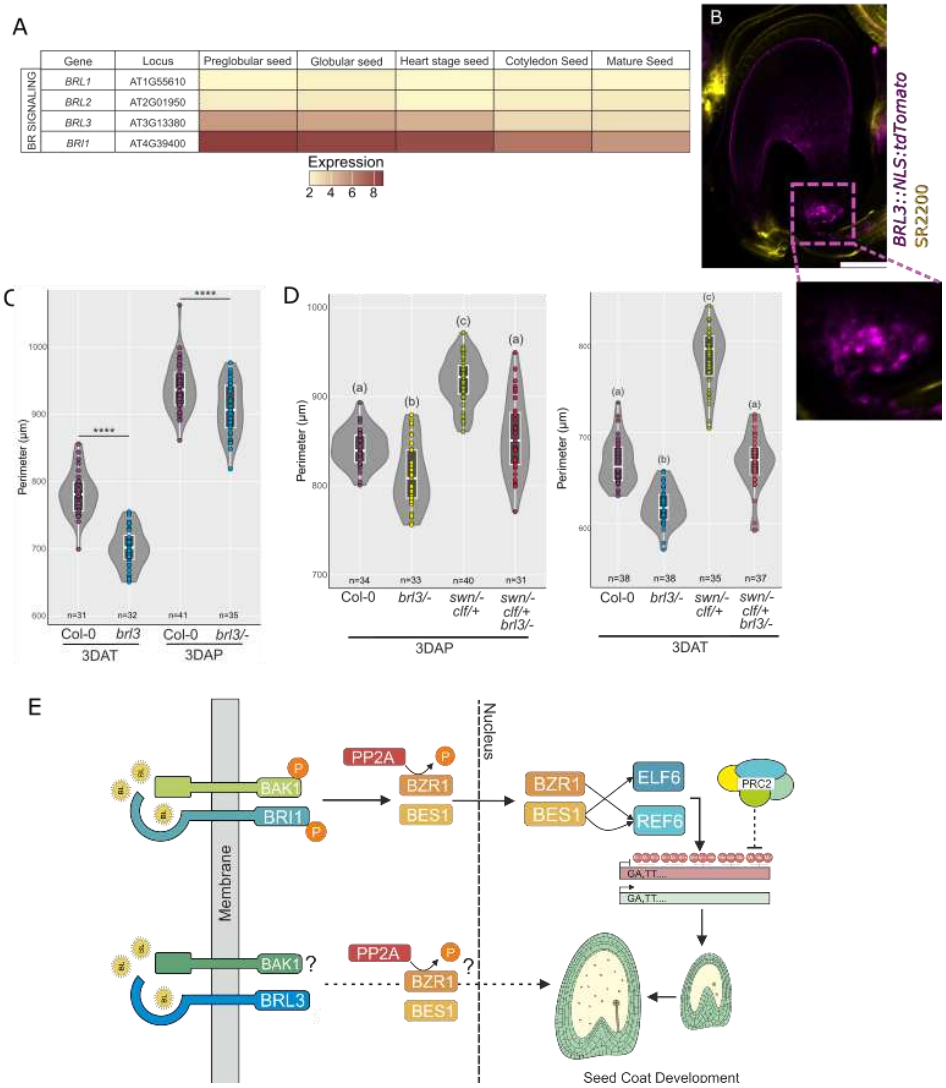

Figure 6. BRL3 regulates seed coat formation independently of H3K27me3. (**A**) Relative expression of BRI-LIKE genes in seed coat, at different stages of seed development, as determined by (Belmonte et al., 2013). (**B**) Expression of a *BRL3::NSL:tdtomato* reporter in a seed at 2 DAP. Yellow is a counterstain with SR2200. Scale bar indicates 50 µm. (**C**) Seed perimeter of Col-0 and *brl3* 3 DAP fertilized and 3 DAT autonomous seeds. **** indicates p-value <0.0001. (Anova). (**D**) Seed perimeter of 3 DAP fertilized and of 3 DAT autonomous seeds of Col-0, *brl3/-*, *swn/- clf/+*, and *swn/- clf/+ brl3/-*. The letters indicate statistical significance for p-value<0.0001 (Anova). (**E**) Working model for our current hypothesis: BR signaling through BRI1 is necessary for removal of H3K27me3 marks from the integuments, priming this tissue for seed coat development. A BRL3-mediated signaling pathway, also dependent on the presence of active BRs is necessary for seed coat growth, in a manner independent of H3K27me3 removal.

Discussion

Deposition of H3K27me3 prevents seed coat development prior to fertilization and these repressive marks must be removed in order for the seed coat to form properly (Figueiredo et al., 2016; Roszak and Köhler, 2011). Our findings support the hypothesis that removal of H3K27me3 is most likely carried out by members of the JMJ family of histone demethylases. Several pieces of evidence support this: first, REF6 and ELF6 are expressed in the integuments and in seed coats. Second, high order *jmj* mutants show seed coat formation defects, including slower relative growth and delayed accumulation of proanthocyanidins, a hallmark of seed coat formation in Arabidopsis (Debeaujon et al., 2003). This phenotype contrasts to that observed in mutants for PRC2, which accumulate proanthocyanidins even without fertilization (Figueiredo et al., 2016), and thus links H3K27me3 removal to seed coat formation.

Moreover, we observed additional reproductive phenotypes in the *elf6 ref6c jmj13* triple mutant, including decreased ovule viability and pollen function, leading to fewer fertilized seeds. This decrease in seed set in the triple mutant siliques may result in more resources being directed towards the remaining seeds, potentially mitigating the putative seed coat defect phenotype found in this triple mutant. Such inverse correlations between seed set and size are well documented in the literature (Jofuku et al., 2005; Ohto et al., 2005). However, we did observe that even single *jmj* mutants produced seeds at maturity that were larger than their WT counterparts, even if their seed set was not much compromised. Our data suggests that zygotic effects from the embryo and the endosperm contribute to this phenotype. Indeed, JMJ function had already been demonstrated in endosperm development: REF6 was shown to remove H3K27me3 marks from the maternal alleles of the endosperm, activating them during germination (Sato et al., 2021). However, we cannot rule out a dual-role of JMJ function in the seed coat, first being necessary

for seed coat initiation, by removal of H3K27me3 marks from the integuments, and later working to repress seed expansion, potentially by targeting different loci at different stages of development. This would fit with REF6 targeting different sets of genes in different stages of seed development.

Given the documented interactions between BR effectors and JMJ demethylases, namely ELF6 and REF6 (Li et al., 2018; Yu et al., 2008), we then assessed the potential role of these steroid hormones in regulating seed coat formation. Based on previously published datasets (Belmonte et al., 2013), BR related genes were predicted to be expressed in seed coats, similar to what happens with *JMJ* genes. We thus hypothesized that BR signaling would be required for JMJ function during seed coat development, allowing for H3K27me3 to be removed from the integuments. In particular, the expression of the BRI1 receptor in the integuments and seed coat, as well as the strong seed coat defects of *bri1*, confirms that BR signaling is required for proper seed coat formation. Both BRI1 and BZR1 were previously shown to be expressed in the integuments during ovule development (Jia et al., 2020). This suggests that BRs are also necessary during ovule development before fertilization. Whether this is via the regulation of H3K27me3 homeostasis or not, is unknown, although it would fit with our observations that lines ectopically expressing *CaMV35S::ELF6* together with *bzr1-D* have severe ovule developmental defects.

Consistent with a role for BR in seed coat formation, BR mutants exhibited smaller seed sizes compared to the WT. Surprisingly, constitutive BR signaling mutants also exhibited smaller seed sizes compared to the WT. These findings suggest that excessive BR signaling has a detrimental effect on seed coat development, indicating a dose-dependent response of BRs in seed coat growth. Similar observations have been made in roots and in endosperms (Lima et al., 2023; Vukašinović et al., 2021). Interestingly, it was previously shown that BES1 is ectopically dephosphorylated in *dwf4-5D,* suggesting increased BR signaling in this gain-of-function mutant (Kim et al., 2013). The reason why *bes1-D* has a negative effect on seed size but *dwf4-5D,* which also presumably has an increased activity of BES1, has a positive effect is still an open question. This dose-dependent mode of action for BRs on seed coat formation was confirmed with exogenous treatments of ovules with epi-BL and with bikinin. For both chemicals, low concentrations had a positive effect on seed coat growth, which was negated at higher concentrations. While the reason for this remains unknown, it is possible that extreme BR levels could result in early or excessive recruitment of ELF6/REF6, resulting in ectopic H3K27me3 demethylation.

Interestingly, BRs have been previously proposed to regulate seed growth and shape in Arabidopsis, via the direct regulation of the endosperm-specific genes *SHB1*, *IKU1*, *MINI3*, and *IKU2*by B ZR1 (Jiang et al., 2013). These genes were thus proposed to regulate seed size downstream of DET2 and BZR1 (Jiang et al., 2013; Jiang and Lin, 2013). However, *MINI3* seems to be also expressed in the sporophytic tissues of the seed (Kang et al., 2013). Alternatively, BZR1 could directly regulate *IKU2* expression (Jiang et al., 2013; Jiang and Lin, 2013), which would require BR signaling to be active in the endosperm. In contrast, our data points to a sporophytic effect on seed size and, furthermore, our reporter analysis places all BR effectors in the seed coat and not the endosperm (Lima et al., 2023). However, we cannot rule out that BR has zygotic effects on seed growth at later stages than the ones we assessed in this study.

We went further to test whether the seed coat defects of BR mutants were indeed linked to poor removal of H3K27me3. Indeed, loss of sporophytic PRC2 alleviates the seed coat defects observed in *bri1*. Notably, *swn/- clf/+ bri1*/- exhibited rescued plant morphologies, including increased leaf size and plant height. This means that many reported phenotypes observed in BR mutants are likely due to altered H3K27me3 homeostasis. Importantly, loss of H3K27me3 in the seed coat is epistatic to the loss of BR signaling via BRI1. This was further confirmed by the observations that the PRC2 mutant was insensitive to exogenous BR applications. A surprising observation came from our analysis of the *swn/- clf/+ det2/-* triple mutant, whose outcome was the opposite of *swn/- clf/+ bri1/-*. Although some rescue of plant morphologies was observed in the triple mutant, it was not as significant as that observed for *bri1*. Moreover, the seed size of *swn/- clf/+ det2/-* remained the same as for the single *det2/-* mutant, indicating that loss of BR biosynthesis is epistatic to loss of PRC2. This suggested that the development of seed coat through BRs may involve multiple pathways, either dependent or independent of the main receptor BRI1. We hypothesized that such an alternative pathway could be under the control of BRLs (Caño-Delgado et al., 2004). Indeed, *brl3* mutants have smaller seeds compared to the WT, and *BRL3* is specifically expressed in the chalazal seed coat. This indicates that BR signaling through BRL3 is involved in seed coat formation. Importantly, the seed coat defects of *brl3* are not rescued by loss of PRC2, unlike what happens for *bri1*. This supports the hypothesis of a BRI1-independent pathway which affects the seed coat growth directly, and not through modulation of H3K27me3 levels. This observation was very interesting because BRI1 and BRL3 are homologous proteins with presumably similar functions. BRL3 was shown to complement the *bri-301* mutant when expressed under the endogenous *BRI1* promoter (Caño-Delgado et al., 2004). It is not known yet if both BRI1 and BRL3 activate the same or different components of BR signaling, but our results show that they might be active in different pathways. It was previously

hypothesized that BES1, which is activated when BRI1 senses BRs, itself seems to act as an activator of BRL3 at low levels of BR, whereas at higher levels, BES1 acts as a repressor of BRL3 in roots (Salazar-Henao et al., 2016).

Overall, our study provides evidence for the involvement of BRs in epigenetic reprogramming during seed coat development in Arabidopsis. The findings suggest that BR signaling is crucial for seed coat growth and that the interplay between BRs, PRC2, and BRL receptors contributes to the intricate regulatory network underlying seed coat formation. We thus propose that: 1) BRI1-mediated BR signaling is necessary for H3K27me3 removal from the integuments, allowing for seed coat formation, and 2) BRI1-independent BR signaling is also necessary for seed coat growth, but in a manner independent of H3K27me3 removal.

Materials and Methods

Plant material and Growth Conditions

The lines used in this study are *elf6-3* (SALK_074694), *elf6-4* (SAIL371D8), *ref6-1* (SALK_001018), *jmj13* (GABI-Kat113B06), *ref6c, elf6-3ref6c, elf6 ref6c jmj13 (ERJ)* and *REF6::REF6:GFP* (Yan et al., 2018), *bri1-6* (Noguchi et al., 1999), *det2* (Chory et al., 1991), *bzr1-D* (Wang et al., 2002), *dwf4-5D* (Kim et al., 2013), *swn-3* (Chanvivattana et al., 2004) *clf-9* (Goodrich et al., 1997) (used as *swn/- clf/+*), *bri1-301* (Xu et al., 2008), *BRI1OX* (Friedrichsen et al., 2000), *bes1-D* (Yin et al., 2002), *cpd91* (SALK_078291), *dwf4-102* (SALK_020761), *dwf5-7* (SALK_127066), *brl3* (SALK_006024), *br6ox1* (SALK_148382) *br6ox2* (SALK_056270), *ROT3::NLS:GFP, DWF4::NLS:GFP*, *BR6OX1::NLS:GFP, BR6OX2::NLS:GFP, BES1::BES1:GFP* (Vukašinović et al., 2021), *BRI1::BRI1:GFP* (Sun et al., 2020), *CYP90A1p:NLS:3xEGFP* (*CPD*) (Vogler et al., 2014), *JMJ13::JMJ13:GFP* (Keyzor et al., 2021), *REF6::REF6*, *TPS1::REF6* and *EPR1::REF6* (Sato et al., 2021). The primer sequences for genotyping mutant lines can be found in **Table S1**.

Seeds were sterilized with 5% commercial bleach with 0.01% Triton X100 for 5 mins followed by 3 times washing with 99.6% ethanol. The sterile seeds were plated onto ½ MS-medium supplemented with 1% sucrose. The plates were kept at 4°C for 48h in the dark for stratification. Plates were then transferred to a growth chamber (16 h light/8 h dark; 50 µmol.s^{-1}.m^{-2}; 22°C). After 10 days, the seedlings were transferred to soil and grown in a growth chamber (16 hr light/8 hr dark; 150 µmol.s^{-1}.m^{-2}; 21/20°C; 70% humidity).

Physiological assays

The hormone treatments used contained 0.1% of ethanol, 0.01% Silwett L-77, and 100 µM of 2,4-Dichlorophenoxyacetic acid (2,4-D). To ensure accuracy in the results, a mock control group was also included in all experiments. Two days prior to anthesis, the flowers were emasculated and two days later were treated with 2,4-D or mock solutions or pollinated. At the designated time intervals, usually three days after treatment (3DAT) or pollination (3DAP), the treated pistils were collected and prepared for microscopy examination.

For clearing of ovules and seeds the whole pistils/siliques were fixed with EtOH:acetic acid (9:1), washed for 10 min in 90% EtOH, 10 min in 70% EtOH and cleared overnight in chloral hydrate solution (66.7% chloral hydrate (w/w), 8.3% glycerol (w/w)). The ovules/seeds were observed under differential interference contrast (DIC) optics using a Leica DM2500 microscope (Leica Microsystems). The DMACA staining was done on 1 DAP, 2 DAP, 3 DAP seeds and 3 DAT autonomous seeds in 2% (w/v) DMACA (p-dimethylaminocinnamaldehyde) in (1:1) 6 N HCl:96% EtOH. The emasculated pistils were incubated in this solution for 30 min and then the ovules/seeds were dissected out and mounted on a microscope slide. Images were recorded using a Leica DM2500 microscope. **Fig. S3** shows the criteria for different levels of DMACA staining. Seed perimeter and area were measured from DIC images using Fiji software. Plots and statistical analysis were done in RStudio.

For fluorescence analysis seeds were mounted in water with 0.1 mg/mL propidium iodide (PI). Samples were analyzed under confocal microscopy on Leica Stellaris 8 Dive with the following settings (in nm; excitation-ex and emission-em): GFP – ex 488, em 500–530; PI – ex 488/514, em 635–719, EYFP (VENUS) – ex 514, em 527. Images were acquired, analyzed and exported using LASX software.

Cloning and generation of transgenic plants

To clone the construct *JMJ13::GFP*, 2300 bps of the *JMJ13* promoter were amplified from Col-0 genomic DNA. The amplified sequence was purified from the gel and was recombined into the donor vector (pDONR221) using BP Gateway cloning according to the manufacturer's instructions (Fisher Scientific). The donor vector was sequenced and the insert recombined into the destination vector pB7FWG.0 using LR Gateway cloning.

To clone *KLUH:BAS1* and *BAN:BAS1*, the *BAS1* coding region was amplified from Col-0 cDNA. The amplified fragments were purified from the gel and were transferred into donor vector pDONR221 using BP Gateway cloning according to the manufacturer's instructions (Fisher Scientific). The donor vector was sequenced to confirm the correct sequence. The donor vector carrying the *BAS1* gene was then recombined into two modified pB7WG2 vectors (VIB, Ghent), where the *CaMV35S* promoter had been replaced with either 4100 bp of the *KLUH* promoter or with 355 bp of the *BANYULS* (*BAN*) promoter.

To clone the constructs for complementation of *bri1* and *det2* mutants, the genomic regions of *BRI1* and *DET2* were amplified from Col-0 genomic DNA. The amplified PCR fragments were purified from the gel and were transferred into donor vector pDONR221 using BP Gateway cloning according to the manufacturer's instructions (Fisher Scientific). Both donor vectors were sequenced and recombined into four modified pB7WG2 vectors using LR Gateway cloning technology. In these destination vectors the *CaMV35S* promoter was replaced with the promoters of the following genes (length of the promoter region indicated in brackets): *DD65* for central cell and early endosperm specific expression (1277 bp), resulting in *DD65:BRI1* and *DD65::DET2* constructs; *BAN* for expression in the endothelium layer of the seed coat (355 bp), resulting in *BAN:BRI1* and *BAN::DET2* constructs; *KLUH* as stronger seed coat specific construct (4100 bp), yielding *KLUH:BRI1* and *KLU::DET2*; and finally *Rps5a* as a constitutively expressed promoter (1613 bp), resulting in constructs *Rps5a:BRI1* and *Rps5a:DET2*.

To clone the constructs for expression analyses of *REF6* and *ELF6*, the pB7WG vector was digested with *Eco*32I and ligated to remove the cassette of the LR reaction. The *GUSplus* reporter gene (Broothaerts et al., 2005) was inserted into *Pst*I and *Bcu*I sites, and the *REF6* and *ELF6* promoter regions (3116 bp and 3002 bp, respectively) were inserted into the *Kpn*I and *Xba*I sites of the vector using the In-Fusion HD Cloning Kit (TaKaRa).

To clone the BRL3 reporter, its promoter was amplified and cloned as a blunt fragment into pJET1.2 (Thermo), and then used to substitute the CaMV35 promoter in pK7WG2 (VIB, Ghent) as a *Spe*I-*Sac*I fragment. Finally, an *NLS:tdTomato* cassette was recombined into that vector via LR Gateway cloning. The ENTRY vector was pEN-L1-NTdTomato-St-L2,0 (VIB, Ghent).

The primer sequences used for cloning can be found in **Table S1**. Multiple independent copies of each construct were transformed into *Agrobacterium tumefaciens* GV3101, and then into *Arabidopsis thaliana* plants using floral dip (Clough and Bent, 1998). The transformants were selected on ½ MS-medium supplemented with 1% sucrose and the appropriate selection agent.

REF6 target prediction

Genes were selected that bear REF6 binding sites, as determined by (Cui et al., 2016), and that were expressed during seed development, as determined by (Belmonte et al., 2013). Only genes bearing four or more CTCTGYTY motifs (N>=4, CTCTGYTY) were included in the analysis. Out of 406 genes meeting this criterion, 326 were expressed in seeds and were used to generate the heatmap of **Fig. S5**. The heatmap was clustered by row with an average Linkage method and Pearson distance measurement method.

Acknowledgments

We thank Kerstin Zander for technical assistance. We thank Jenny Russinova for providing several reporter lines for BR biosynthesis genes as well as BR mutants, Jurgen Kleine-Vehn for the BRI1 reporter, Kerstin Kaufmann for JMJ mutants and REF6 reporter, Juthamas Chaiwanon for *det2*, Sunghwa Choe for *dwf4-5D* and Jie Song for the *JMJ13* reporter and the *CaMV35S::ELF6* line. We also thank Kian Hématy, Juthamas Chaiwanon and Kamil Ruzicka for additional reporter lines, which finally were not included in the manuscript.

This work was funded by project number 421178202 of the German Research Foundation (DFG) to DDF, the Human Frontier Science Program (LT000162/2018-L) to HS, and by the Max Planck Society.

Author contributions

RP, RBL, GYL and DDF designed the study. RP, RBL, GYL, SE and HS performed the experiments. RP and GYL analyzed the data. RP and DDF wrote the first draft of the manuscript, and all authors contributed to and approved the final version.

References

Adamski NM, Anastasiou E, Eriksson S, O'Neill CM, Lenhard M. 2009. Local maternal control of seed size by KLUH/CYP78A5-dependent growth signaling. *Proc Natl Acad Sci U S A* **106**:20115–20120. doi:DOI 10.1073/pnas.0907024106

Belmonte MF, Kirkbride RC, Stone SL, Pelletier JM, Bui AQ, Yeung EC, Hashimoto M, Fei J, Harada CM, Munoz MD, Le BH, Drews GN, Brady SM, Goldberg RB, Harada JJ. 2013.

Comprehensive developmental profiles of gene activity in regions and subregions of the Arabidopsis seed. *Proceedings of the National Academy of Sciences* **110**:E435–E444. doi:10.1073/pnas.1222061110

Borg M, Jacob Y, Susaki D, LeBlanc C, Buendía D, Axelsson E, Kawashima T, Voigt P, Boavida L, Becker J, Higashiyama T, Martienssen R, Berger F. 2020. Targeted reprogramming of H3K27me3 resets epigenetic memory in plant paternal chromatin. *Nat Cell Biol* **22**:621–629. doi:10.1038/s41556-020-0515-y

Broothaerts W, Mitchell HJ, Weir B, Kaines S, Smith LMA, Yang W, Mayer JE, Roa-Rodríguez C, Jefferson RA. 2005. Gene transfer to plants by diverse species of bacteria. *Nature* **433**:629–633. doi:10.1038/nature03309

Caño-Delgado A, Yin Y, Yu C, Vafeados D, Mora-García S, Cheng J-C, Nam KH, Li J, Chory J. 2004. BRL1 and BRL3 are novel brassinosteroid receptors that function in vascular differentiation in *Arabidopsis*. *Development* **131**:5341–5351. doi:10.1242/dev.01403

Chanvivattana Y, Bishopp A, Schubert D, Stock C, Moon Y-H, Sung ZR, Goodrich J. 2004. Interaction of Polycomb-group proteins controlling flowering in *Arabidopsis*. *Development* **131**:5263–5276. doi:10.1242/dev.01400

Chen H, Tong J, Fu W, Liang Z, Ruan J, Yu Y, Song X, Yuan L, Xiao L, Liu J, Cui Y, Huang S, Li C. 2020. The H3K27me3 Demethylase RELATIVE OF EARLY FLOWERING6 Suppresses Seed Dormancy by Inducing Abscisic Acid Catabolism. *Plant Physiology* **184**:1969–1978. doi:10.1104/pp.20.01255

Choe S, Tanaka A, Noguchi T, Fujioka S, Takatsuto S, Ross AS, Tax FE, Yoshida S, Feldmann KA. 2000. Lesions in the sterol Δ7 reductase gene of Arabidopsis cause dwarfism due to a block in brassinosteroid biosynthesis. *The Plant Journal* **21**:431–443. doi:10.1046/j.1365-313x.2000.00693.x

Chory J, Nagpal P, Peto CA. 1991. Phenotypic and Genetic Analysis of det2, a New Mutant That Affects Light-Regulated Seedling Development in Arabidopsis. *Plant Cell* 445–459. doi:10.1105/tpc.3.5.445

Clough SJ, Bent AF. 1998. Floral dip: a simplified method for Agrobacterium-mediated transformation of Arabidopsis thaliana. *Plant J* **16**:735–743. doi:10.1046/j.1365-313x.1998.00343.x

Crevillén P. 2020. Histone Demethylases as Counterbalance to H3K27me3 Silencing in Plants. *iScience* **23**:101715. doi:10.1016/j.isci.2020.101715

Crevillén P, Yang H, Cui X, Greeff C, Trick M, Qiu Q, Cao X, Dean C. 2014. Epigenetic reprogramming that prevents transgenerational inheritance of the vernalized state. *Nature* **515**:587–590.

Cui Xia, Lu F, Qiu Q, Zhou B, Gu L, Zhang S, Kang Y, Cui Xiekui, Ma X, Yao Q, Ma J, Zhang X, Cao X. 2016. REF6 recognizes a specific DNA sequence to demethylate H3K27me3 and regulate organ boundary formation in Arabidopsis. *Nat Genet* **48**:694–699. doi:10.1038/ng.3556

Debeaujon I, Nesi N, Perez P, Devic M, Grandjean O, Caboche M, Lepiniec L. 2003. Proanthocyanidin-accumulating cells in Arabidopsis testa: regulation of differentiation and role in seed development. *Plant Cell* **15**:2514–2531. doi:10.1105/tpc.014043

Fàbregas N, Caño-Delgado AI. 2014. Turning on the microscope turret: a new view for the study of brassinosteroid signaling in plant development. *Physiologia plantarum* **151**:172–183.

Figueiredo DD, Batista RA, Roszak PJ, Hennig L, Köhler C. 2016. Auxin production in the endosperm drives seed coat development in Arabidopsis. *eLife* **5**:1–23. doi:10.7554/eLife.20542

Figueiredo DD, Batista RA, Roszak PJ, Köhler C. 2015. Auxin production couples endosperm development to fertilization. *Nat Plants* **1**:15184. doi:10.1038/nplants.2015.184

Friedrichsen DM, Joazeiro CAP, Li J, Hunter T, Chory J. 2000. Brassinosteroid-Insensitive-1 Is a Ubiquitously Expressed Leucine-Rich Repeat Receptor Serine/Threonine Kinase.

Plant Physiology **123**:1247–1256. doi:10.1104/pp.123.4.1247

Fukuta N, Fukuzono K, Kawaide H, Abe H, Nakayama M. 2006. Physical Restriction of Pods Causes Seed Size Reduction of a Brassinosteroid-deficient Faba Bean (Vicia faba). *Annals of Botany* **97**:65–69. doi:10.1093/aob/mcj014

Gan E-S, Xu Y, Wong J-Y, Goh JG, Sun B, Wee W-Y, Huang J, Ito T. 2014. Jumonji demethylases moderate precocious flowering at elevated temperature via regulation of FLC in Arabidopsis. *Nat Commun* **5**:5098. doi:10.1038/ncomms6098

Garcia D, Saingery V, Chambrier P, Mayer U, Jurgens G, Berger F. 2003. Arabidopsis haiku mutants reveal new controls of seed size by endosperm. *Plant physiology* **131**:1661–1670.

Goodrich J, Puangsomlee P, Martin M, Long D, Meyerowitz EM, Coupland G. 1997. A Polycomb-group gene regulates homeotic gene expression in Arabidopsis. *Nature* **386**:44–51. doi:10.1038/386044a0

Hartwig T, Corvalan C, Best NB, Budka JS, Zhu JY, Choe S, Schulz B. 2012. Propiconazole is a specific and accessible brassinosteroid (BR) biosynthesis inhibitor for arabidopsis and maize. *PLoS ONE* **7**. doi:10.1371/journal.pone.0036625

Hemenway EA, Gehring M. 2023. Epigenetic Regulation During Plant Development and the Capacity for Epigenetic Memory. *Annu Rev Plant Biol* **74**:87–109. doi:10.1146/annurev-arplant-070122-025047

Hong Z, Ueguchi-Tanaka M, Fujioka S, Takatsuto S, Yoshida S, Hasegawa Y, Ashikari M, Kitano H, Matsuoka M. 2005. The Rice brassinosteroid-deficient dwarf2 Mutant, Defective in the Rice Homolog of Arabidopsis DIMINUTO/DWARF1, Is Rescued by the Endogenously Accumulated Alternative Bioactive Brassinosteroid, Dolichosterone. *The Plant Cell* **17**:2243–2254. doi:10.1105/tpc.105.030973

Jia D, Chen L-G, Yin G, Yang X, Gao Z, Guo Y, Sun Y, Tang W. 2020. Brassinosteroids regulate outer ovule integument growth in part via the control of INNER NO OUTER by BRASSINOZOLE-RESISTANT family transcription factors. *Journal of Integrative Plant Biology* **62**:1093–1111. doi:10.1111/jipb.12915

Jiang W-B, Huang H-Y, Hu Y-W, Zhu S-W, Wang Z-Y, Lin W-H. 2013. Brassinosteroid Regulates Seed Size and Shape in Arabidopsis. *Plant Physiology* **162**:1965–1977. doi:10.1104/pp.113.217703

Jiang W-B, Lin W-H. 2013. Brassinosteroid functions in Arabidopsis seed development. *Plant Signaling & Behavior* **8**:e25928. doi:10.4161/psb.25928

Jofuku KD, Omidyar PK, Gee Z, Okamuro JK. 2005. Control of seed mass and seed yield by the floral homeotic gene *APETALA2*. *Proc Natl Acad Sci USA* **102**:3117–3122. doi:10.1073/pnas.0409893102

Kang X, Li W, Zhou Y, Ni M. 2013. A WRKY Transcription Factor Recruits the SYG1-Like Protein SHB1 to Activate Gene Expression and Seed Cavity Enlargement. *PLoS Genet* **9**:e1003347. doi:10.1371/journal.pgen.1003347

Keyzor C, Mermaz B, Trigazis E, Jo S, Song J. 2021. Histone Demethylases ELF6 and JMJ13 Antagonistically Regulate Self-Fertility in Arabidopsis. *Frontiers in Plant Science* **12**.

Kim B, Fujioka S, Kwon M, Jeon J, Choe S. 2013. Arabidopsis brassinosteroid-overproducing gulliver3-D/dwarf4-D mutants exhibit altered responses to jasmonic acid and pathogen. *Plant Cell Rep* **32**:1139–1149. doi:10.1007/s00299-012-1381-2

Li Z, Ou Y, Zhang Z, Li J, He Y. 2018. Brassinosteroid Signaling Recruits Histone 3 Lysine-27 Demethylation Activity to FLOWERING LOCUS C Chromatin to Inhibit the Floral Transition in Arabidopsis. *Mol Plant* **11**:1135–1146. doi:10.1016/j.molp.2018.06.007

Lima RB, Pankaj R, Ehlert S, Finger P, Fröhlich A, Bayle V, Landrein B, Sampathkumar A, Figueiredo DD. 2023. Seed coat-derived brassinosteroids non-cell autonomously regulate endosperm development (preprint). Research Square. doi:10.21203/rs.3.rs-3673733/v1

Lu F, Cui X, Zhang S, Jenuwein T, Cao X. 2011. Arabidopsis REF6 is a histone H3 lysine 27 demethylase. *Nat Genet* **43**:715–719. doi:10.1038/ng.854

Lu SX, Knowles SM, Webb CJ, Celaya RB, Cha C, Siu JP, Tobin EM. 2011. The Jumonji C domain-containing protein JMJ30 regulates period length in the Arabidopsis circadian clock. *Plant Physiol* **155**:906–915. doi:10.1104/pp.110.167015

Luo M, Dennis ES, Berger F, Peacock WJ, Chaudhury A. 2005. *MINISEED3* (*MINI3*), a *WRKY* family gene, and *HAIKU2* (*IKU2*), a leucine-rich repeat (*LRR*) *KINASE* gene, are regulators of seed size in *Arabidopsis*. *Proc Natl Acad Sci USA* **102**:17531–17536. doi:10.1073/pnas.0508418102

Lv B, Tian H, Zhang F, Liu J, Lu S, Bai M, Li C, Ding Z. 2018. Brassinosteroids regulate root growth by controlling reactive oxygen species homeostasis and dual effect on ethylene synthesis in Arabidopsis. *PLoS Genetics* **14**:e1007144.

Manghwar H, Hussain A, Ali Q, Liu F. 2022. Brassinosteroids (BRs) Role in Plant Development and Coping with Different Stresses. *IJMS* **23**:1012. doi:10.3390/ijms23031012

Maruyama D, Hamamura Y, Takeuchi H, Susaki D, Nishimaki M, Kurihara D, Kasahara RD, Higashiyama T. 2013. Independent Control by Each Female Gamete Prevents the Attraction of Multiple Pollen Tubes. *Developmental Cell* **25**:317–323. doi:10.1016/j.devcel.2013.03.013

Morinaka Y, Sakamoto T, Inukai Y, Agetsuma M, Kitano H, Ashikari M, Matsuoka M. 2006. Morphological Alteration Caused by Brassinosteroid Insensitivity Increases the Biomass and Grain Production of Rice. *Plant Physiology* **141**:924–931. doi:10.1104/pp.106.077081

Mozgova I, Köhler C, Hennig L. 2015. Keeping the gate closed: functions of the polycomb repressive complex PRC2 in development. *The Plant Journal* **83**:121–132. doi:10.1111/tpj.12828

Noguchi T, Fujioka S, Choe S, Takatsuto S, Yoshida S, Yuan H, Feldmann KA, Tax FE. 1999. Brassinosteroid-Insensitive Dwarf Mutants of Arabidopsis Accumulate Brassinosteroids. *Plant Physiology* **121**:743–752. doi:10.1104/pp.121.3.743

Nomura T, Ueno M, Yamada Y, Takatsuto S, Takeuchi Y, Yokota T. 2007. Roles of Brassinosteroids and Related mRNAs in Pea Seed Growth and Germination. *Plant Physiology* **143**:1680–1688. doi:10.1104/pp.106.093096

Ohto M, Fischer RL, Goldberg RB, Nakamura K, Harada JJ. 2005. Control of seed mass by *APETALA2*. *Proc Natl Acad Sci USA* **102**:3123–3128. doi:10.1073/pnas.0409858102

Pan J, Zhang H, Zhan Z, Zhao T, Jiang D. 2023. A REF6-dependent H3K27me3-depleted state facilitates gene activation during germination in Arabidopsis. *Journal of Genetics and Genomics* **50**:178–191. doi:10.1016/j.jgg.2022.09.001

Roszak P, Köhler C. 2011. Polycomb group proteins are required to couple seed coat initiation to fertilization. *Proc Natl Acad Sci USA* **108**:20826–20831. doi:10.1073/pnas.1117111108

Rybel BD, Audenaert D, Vert G, Rozhon W, Mayerhofer J, Peelman F, Coutuer S, Denayer T, Jansen L, Nguyen L, Vanhoutte I, Beemster GTS, Vleminckx K, Jonak C, Chory J, Inzé D, Russinova E, Beeckman T. 2009. Chemical Inhibition of a Subset of Arabidopsis thaliana GSK3-like Kinases Activates Brassinosteroid Signaling. *Chemistry and Biology* **16**:594–604. doi:10.1016/j.chembiol.2009.04.008

Salazar-Henao JE, Lehner R, Betegón-Putze I, Vilarrasa-Blasi J, Caño-Delgado AI. 2016. BES1 regulates the localization of the brassinosteroid receptor BRL3 within the provascular tissue of the Arabidopsis primary root. *Journal of Experimental Botany* **67**:4951–4961. doi:10.1093/jxb/erw258

Sato H, Santos-González J, Köhler C. 2021. Combinations of maternal-specific repressive epigenetic marks in the endosperm control seed dormancy. *eLife* **10**:e64593. doi:10.7554/eLife.64593

933 Singh AP, Savaldi-Goldstein S. 2015. Growth control: brassinosteroid activity gets context.
934 *Journal of experimental botany* **66**:1123–1132.
935 Stadler R, Lauterbach C, Sauer N. 2005. Cell-to-cell movement of green fluorescent protein
936 reveals post-phloem transport in the outer integument and identifies symplastic domains
937 in Arabidopsis seeds and embryos. *Plant Physiology* **139**:701–712.
938 doi:10.1104/pp.105.065607
939 Steffen JG, Kang IH, Macfarlane J, Drews GN. 2007. Identification of genes expressed in the
940 Arabidopsis female gametophyte. *Plant Journal* **51**:281–292. doi:10.1111/j.1365-
941 313X.2007.03137.x
942 Sun L, Feraru E, Feraru MI, Waidmann S, Wang W, Passaia G, Wang Z-Y, Wabnik K, Kleine-
943 Vehn J. 2020. PIN-LIKES Coordinate Brassinosteroid Signaling with Nuclear Auxin Input
944 in Arabidopsis thaliana. *Current Biology* **30**:1579-1588.e6.
945 doi:10.1016/j.cub.2020.02.002
946 Takahashi N, Nakazawa M, Shibata K, Yokota T, Ishikawa A, Suzuki K, Kawashima M,
947 Ichikawa T, Shimada H, Matsui M. 2005. shk1-D, a dwarf Arabidopsis mutant caused by
948 activation of the CYP72C1 gene, has altered brassinosteroid levels. *The Plant Journal*
949 **42**:13–22. doi:10.1111/j.1365-313X.2005.02357.x
950 Tanabe S, Ashikari M, Fujioka S, Takatsuto S, Yoshida S, Yano M, Yoshimura A, Kitano H,
951 Matsuoka M, Fujisawa Y, Kato H, Iwasaki Y. 2005. A Novel Cytochrome P450 Is
952 Implicated in Brassinosteroid Biosynthesis via the Characterization of a Rice Dwarf
953 Mutant, dwarf11, with Reduced Seed Length. *The Plant Cell* **17**:776–790.
954 doi:10.1105/tpc.104.024950
955 Turk EM, Fujioka S, Seto H, Shimada Y, Takatsuto S, Yoshida S, Wang H, Torres QI, Ward JM,
956 Murthy G, Zhang J, Walker JC, Neff MM. 2005. *BAS1* and *SOB7* act redundantly to
957 modulate Arabidopsis photomorphogenesis via unique brassinosteroid inactivation
958 mechanisms. *The Plant Journal* **42**:23–34. doi:10.1111/j.1365-313X.2005.02358.x
959 Vogler F, Schmalzl C, Englhart M, Bircheneder M, Sprunck S. 2014. Brassinosteroids promote
960 Arabidopsis pollen germination and growth. *Plant Reprod* **27**:153–167.
961 doi:10.1007/s00497-014-0247-x
962 Vukašinović N, Wang Y, Vanhoutte I, Fendrych M, Guo B, Kvasnica M, Jiroutová P, Oklestkova
963 J, Strnad M, Russinova E. 2021. Local brassinosteroid biosynthesis enables optimal root
964 growth. *Nat Plants* **7**:619–632. doi:10.1038/s41477-021-00917-x
965 Vukašinović N, Wang Y, Vanhoutte I, Fendrych M, Kvasnica M, Jiroutová P, Oklestkova J,
966 Strnad M. n.d. Local brassinosteroid biosynthesis enables optimal root growth.
967 Wang A, Garcia D, Zhang H, Feng K, Chaudhury A, Berger F, Peacock WJ, Dennis ES, Luo M.
968 2010. The VQ motif protein IKU1 regulates endosperm growth and seed size in
969 Arabidopsis: IKU1, a VQ motif protein, regulates seed size. *The Plant Journal* **63**:670–
970 679. doi:10.1111/j.1365-313X.2010.04271.x
971 Wang Q, Yu F, Xie Q. 2020. Balancing growth and adaptation to stress: Crosstalk between
972 brassinosteroid and abscisic acid signaling. *Plant, Cell & Environment* **43**:2325–2335.
973 Wang Yahan, Gu D, Deng L, He C, Zheng F, Liu X. 2023. The Histone H3K27 Demethylase
974 REF6 Is a Positive Regulator of Light-Initiated Seed Germination in Arabidopsis. *Cells*
975 **12**:295. doi:10.3390/cells12020295
976 Wang Yaowei, Perez-Sancho J, Platre MP, Callebaut B, Smokvarska M, Ferrer K, Luo Y, Nolan
977 TM, Sato T, Busch W, Benfey PN, Kvasnica M, Winne JM, Bayer EM, Vukašinović N,
978 Russinova E. 2023. Plasmodesmata mediate cell-to-cell transport of brassinosteroid
979 hormones. *Nat Chem Biol*. doi:10.1038/s41589-023-01346-x
980 Wang ZY, Nakano T, Gendron J, He J, Chen M, Vafeados D, Yang Y, Fujioka S, Yoshida S,
981 Asami T, Chory J. 2002. Nuclear-localized BZR1 mediates brassinosteroid-induced
982 growth and feedback suppression of brassinosteroid biosynthesis. *Developmental Cell*.
983 doi:10.1016/S1534-5807(02)00153-3

Wu C, Trieu A, Radhakrishnan P, Kwok SF, Harris S, Zhang K, Wang J, Wan J, Zhai H, Takatsuto S, Matsumoto S, Fujioka S, Feldmann KA, Pennell RI. 2008. Brassinosteroids Regulate Grain Filling in Rice. *The Plant Cell* **20**:2130–2145. doi:10.1105/tpc.107.055087

Xu W, Huang J, Li B, Li J, Wang Y. 2008. Is kinase activity essential for biological functions of BRI1? *Cell Res* **18**:472–478. doi:10.1038/cr.2008.36

Yan W, Chen D, Smaczniak C, Engelhorn J, Liu H, Yang W, Graf A, Carles CC, Zhou D-X, Kaufmann K. 2018. Dynamic and spatial restriction of Polycomb activity by plant histone demethylases. *Nature plants* **4**:681–689.

Yang H, Howard M, Dean C. 2016. Physical coupling of activation and derepression activities to maintain an active transcriptional state at FLC. *Proc Natl Acad Sci U S A* **113**:9369–9374. doi:10.1073/pnas.1605733113

Yin Y, Wang Z-Y, Mora-Garcia S, Li J, Yoshida S, Asami T, Chory J. 2002. BES1 Accumulates in the Nucleus in Response to Brassinosteroids to Regulate Gene Expression and Promote Stem Elongation. *Cell* **109**:181–191. doi:10.1016/S0092-8674(02)00721-3

Yu X, Li Li, Li Lei, Guo M, Chory J, Yin Y. 2008. Modulation of brassinosteroid-regulated gene expression by jumonji domain-containing proteins ELF6 and REF6 in Arabidopsis. *Proceedings of the National Academy of Sciences of the United States of America* **105**:7618–7623. doi:10.1073/pnas.0802254105

Zhou Y, Zhang Xiaojuan, Kang X, Zhao X, Zhang Xiansheng, Ni M. 2009. SHORT HYPOCOTYL UNDER BLUE1 Associates with MINISEED3 and HAIKU2 Promoters in Vivo to Regulate Arabidopsis Seed Development. *The Plant Cell* **21**:106–117. doi:10.1105/tpc.108.064972